DISCLAIMER NOTICE

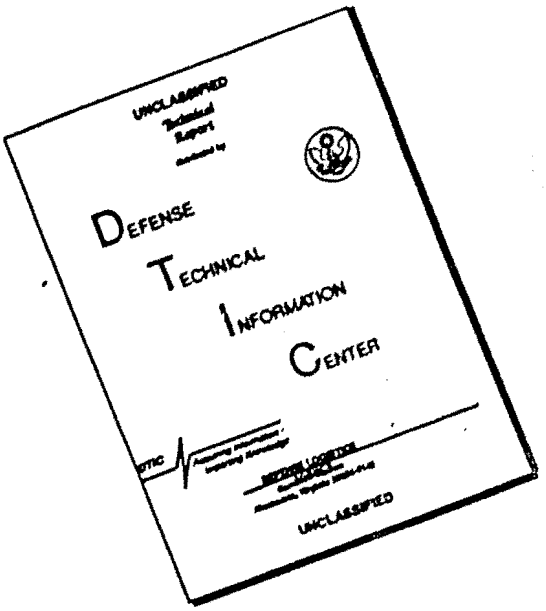

THIS DOCUMENT IS BEST QUALITY AVAILABLE. THE COPY FURNISHED TO DTIC CONTAINED A SIGNIFICANT NUMBER OF PAGES WHICH DO NOT REPRODUCE LEGIBLY.

THE MANCHESTER COLLEGE OF SCIENCE AND TECHNOLOGY

Department of Textile Technology

MECHANICAL BEHAVIOUR OF TWISTED YARNS

1. Fatigue behaviour of twisted continuous filament yarns

By

A.J.Booth and J.W.S.Hearle

U.S.Army Contract Number
DA-91-591-EUC-~~1467~~ 1116
01-4601-60

Final Technical Report. October 1962-October 1963

"The research reported in this document has been made possible through the support and sponsorship of the U.S.Department of Army, through its European Research Office."

TO: European Research Office (8671 DU)
U.S.Department of Army
2 Rheingau Allee
Frankfurt/Main
G E R M A N Y

To be mailed to:

U.S.Army R.& D.
Liaison Group (9851DU)
APO 757
U.S.Forces (Europe)

(Report due: October 31st 1963)

This Final Technical report has been taken from the full report of the three years' investigation into the subject of the fatigue behaviour of twisted continuous filaments and consequently the numbering of chapters and pages do not start from unity.

ACKNOWLEDGEMENTS

The author wishes to express his gratitude to Professor J.J.Vincent, M.Sc., F.T.I., for his interest in the work; to Dr.J.W.S.Hearle, M.A., Ph.D., A.Inst.P., for his sustained guidance and valued contribution to the study.

Thanks are also due to all members of staff who have contributed to the presentation of this report and in particular to Miss B.Stacey for invaluable help in preparation of the majority of the diagrams and to Miss S.Larkin for her typing of the report.

The construction of the two fatigue testers and auxiliary apparatus was greatly aided by the advice and practical help of Mr.D.J.Clarke.

Sincere thanks are due to the European Research Office of the United States Department of the Army for their generous financial support, which has made the present work possible.

Last but by no means least, thanks are offered to all the many research colleagues for their assistance and interest shown during the whole course of the study.

SUMMARY

The second fatigue tester, described fully in the Annual report of October 1961-October 1962 has been used, after minor modifications, to provide information of the fatigue behaviour of four textile materials at six ranges of twist and three stroke levels. Analysis of the results has been split into three sections which deal respectively with the optical appearance of fractured specimens, the statistical nature of fatigue breakage, and the possibility of predicting fatigue failure by means of the known elastic recovery properties of the material.

C O N T E N T S

THE FATIGUE PROPERTIES OF TWISTED CONTINUOUS FILAMENT YARNS

CHAPTER 4

GENERAL REVIEW OF EARLIER WORK

4.1. Introduction

In the first annual report[+] the description of a fixed extension fatigue tester and the results obtained with it have been presented; the second annual report[*] gives details of the design and construction of the cumulative extension fatigue tester whereby slack is removed at the end of each cycle. A few results were presented; this report gives the results together with the analysis and interpretation for the whole testing programme.

In the cumulative extension tester, specimens, 10 cm. in length, are mounted between the pairs of jaws. The upper jaws are fixed to stiff phosphor bronze beams fitted with resistance strain gauges so that the tension in a specimen can be detected and recorded. The phosphor bronze beams are mounted on a bar which is subjected to an adjustable sinusoidal displacement by means of a reciprocating mechanism attached to the main drive. The lower jaws are attached to brass rods which pass through a clamping device operated by electromagnets. The clamps are opened 15° before the upper jaws are in their lowest position in order to allow the slack to be taken up,

---

[+] U.S.Army Contract Number DA-91-591-EUC-1467-01-4601-60
Final Technical Report October 1960-October 1961

[*] U.S.Army Contract Number DA-91-591-EUC-1467-01-4601-60
Final Technical Report October 1961-October 1962

and reclosed 15° after the lowest position. Fixed to the lower ends of the brass rods are soft iron rods which extend into the coils of a mutual inductance. The change in mutual inductance can be detected, recorded and used as a measure of the cumulative extension of the specimen. In order to prevent untwisting of the yarns, needles are fixed transversely to the lower jaws and passed between guide rods. The total mass of the lower jaw assembly is 8.3 g: this makes up the mutual pretension used for mounting and the tension used to take up slack after each cycle. When a specimen breaks, the lower jaw assembly drops down, and operates a microswitch which stops a counter so that the number of cycles to break is recorded. The tests were carried out at a frequency of 61 cycles per minute. All tests were carried out in a controlled atmosphere of 65% r.h. and 20°C.

4.2. Modifications Subsequent to the Last Report

Improvements of the machine since its initial commissioning has taken place in the following ways:

(a) Mechanical stability of the reciprocating movement.

(b) Modification of the clamping mechanism to give greater reliability over long running periods.

Regarding the first point, it was found that although the system referred to in the last report worked adequately, there was a marked tendency for the peak of the cycle to be flattened excessively and the departure from the true sine wave to become serious. This was particularly noticeable at high strokes where the ratio of lengths of connecting rod to effective crank radius became relatively small.

Another disadvantage of the first system employed was that the reciprocating rods were constrained to pass through $\frac{1}{2}$" reamed holes in brass housings and although the movement was also constrained by the small pulleys running in tracks, it was found that wear and consequent looseness in the $\frac{1}{2}$" holes occurred and this resulted in occasional stick-slip motion which could not be tolerated.

Fig.69 shows the new system which has been evolved. A and B are Ransome and Marles $\frac{1}{2}$" linear bearings which are in housings screwed to the base plate. As can be seen, the distance from C to D has been considerably increased and this has effectively prevented flattening of the sine wave. The movement is also much smoother and providing it is maintained regularly with the help of a little molybdenum disulphide grease on the ball races, it is capable of running non-stop for very long periods.

The steel pin shown at the top of Fig.69 is adjustable with respect to a steel disc, keyed on to the mainshaft. The eccentric disc has the 3/16" dia. pin at its centre and this pin supports the weight of the reciprocating movement.

The distance of the centre of the pin from the centre of the mainshaft can be varied between 0 and 1.25 cm, which facilitates strokes of up to 25% of the gauge length. A millimetre scale is screwed to the disc and it is possible to set the stroke to better than 0.1%.

The second improvement which has been found necessary is alteration of the method of clamping, although the principle remains

FIG. 69.

THE MODIFIED RECIPROCATING MECHANISM.

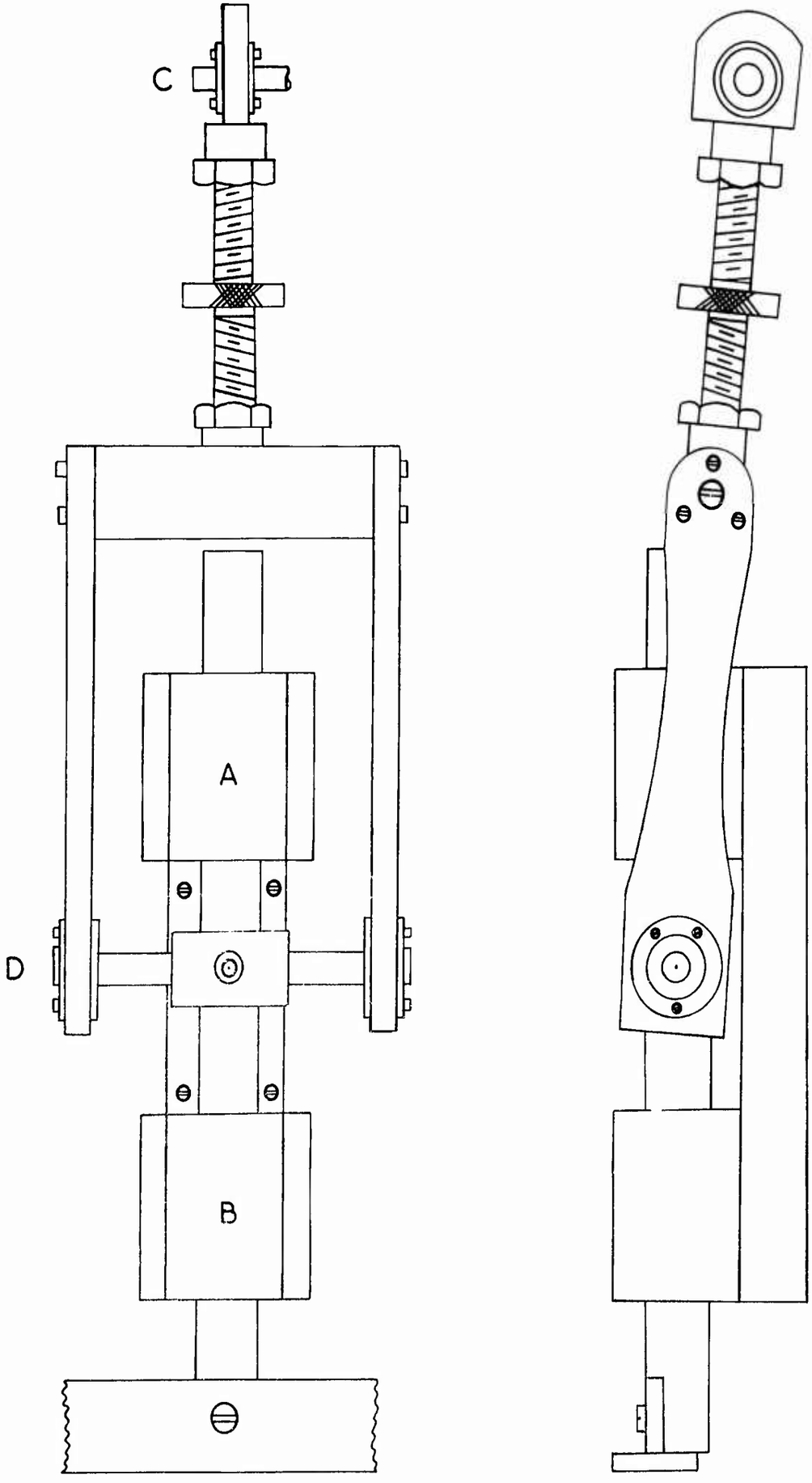

the same as previously. It was found, particularly at high strokes, that it became increasingly difficult to clamp the 20 brass rods simultaneously over a length of almost 3 feet. This system used 3 electromagnets; the present system uses 4 electromagnets and the bank of stations has been split into two sections of 8 stations each. It is found that clamping is greatly improved. The new system does, however, mean a drop of 20% in the number of stations being used.

Another problem which arises with long period running of the machine is that of overheating of the electromagnets, the design of which incorporates a wax used for insulation purposes. After long running times, the melting of this wax was found very troublesome and its removal entailed stripping down the electromagnets and a thorough clean with either carbon tetrachloride or trichloroethylene.

It was decided that a cooling system could be used to remedy this difficulty and a jacket consisting of 3/32" bore copper tubing has been constructed and fitted in close proximity to each of the four electromagnets.

A slow flow of water is fed through the system, arranged in series, and on a spot check the temperature of the water was found to have risen by 8°C. during passage through the system.

A photograph of the tester with these modifications having been carried out is shown in Fig.70. The control board is also shown.

FIG. 70 THE SECOND FATIGUE TESTER (AFTER MODIFICATION)

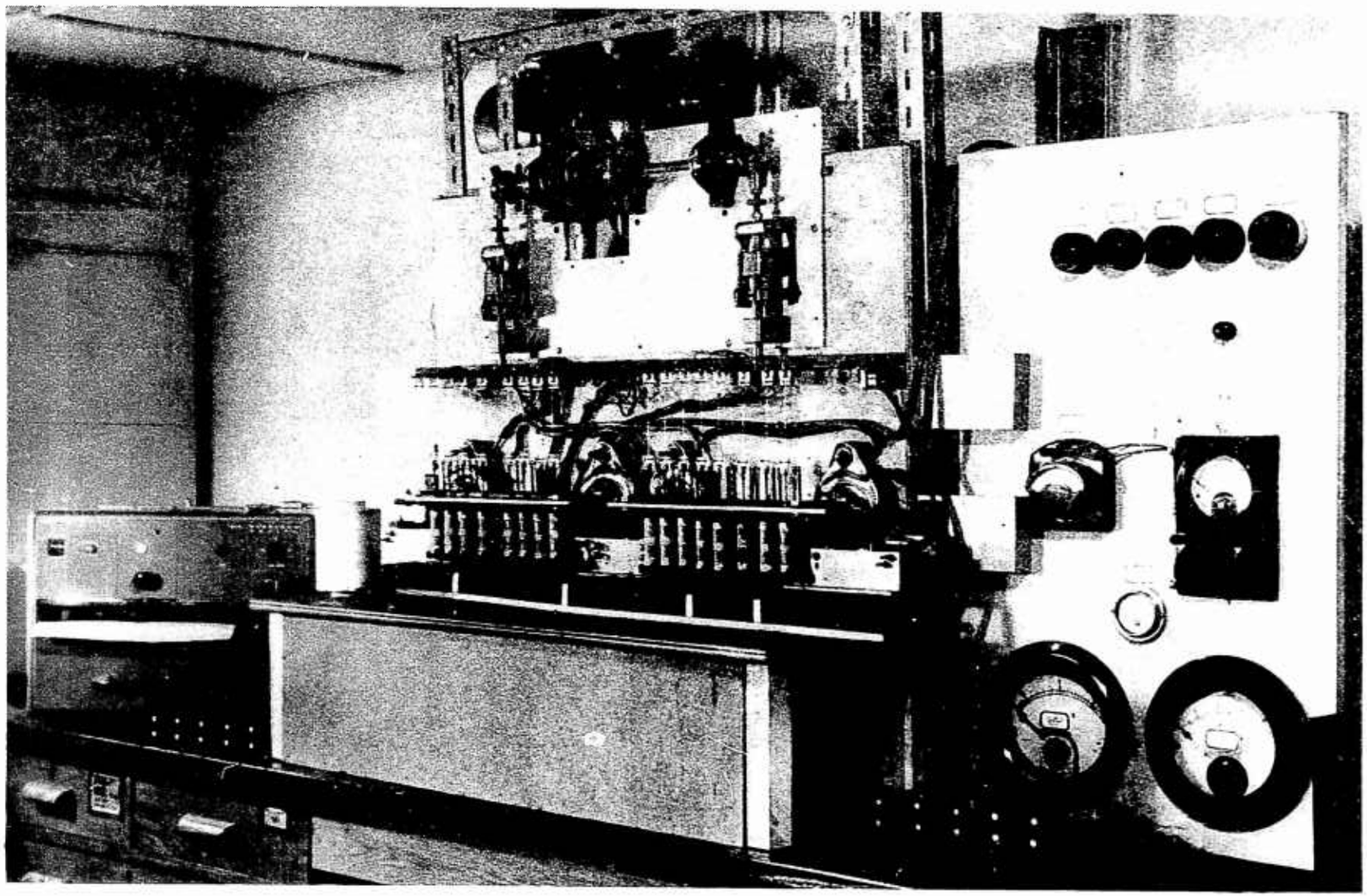

CHAPTER 5

EXPERIMENTAL RESULTS

5.1. Choice of Strokes of Testing

After preliminary experiments had been made and the behaviour of the various types of material under fatigue conditions had been studied, the strokes given in Table XXVI were used for the yarns shown.

TABLE XXVI

		Stroke %					
		$2\frac{1}{2}$	5	$7\frac{1}{2}$	10	$12\frac{1}{2}$	15
NOMINAL	0	VA	VA	T	VANT	NT	N
T.P.I.	10	VA	VA	T	VANT	NT	N
	20	VA	VA	T	VANT	NT	N
	30	VA	VA	T	VANT	NT	N
	45	VA	VA	T	VANT	NT	N
	65	VA	VA	T	VANT	NT	N

V Viscose N Nylon

A Acetate T Terylene

The three main variables associated with the tests are the stress, the instantaneous length and the number of cycles to break. These three variables have been found for each of the insertions in the table above.

5.2. A Typical Record Chart

A typical trace from which readings of tension and length are made is shown in Fig.71. As can be seen three galvanometers are being used, one for length measurements (A.C. 50 c/s), one for

tension measurements (modified D.C. sine wave) and a third as a timing trace. The frequency of this trace is 61 cycles per minute and for clarity of reproduction the A.C. signal has been reduced in the diagram to one third of its actual frequency.

When the electromagnetic clamps open, indicated by the sharp fall in the timing trace, it can be seen that there is a short time lag (approximately 70 milliseconds) before the lower jaw assembly falls to its new position. This is also shown up by the impact tension on the yarn at this point which amounts to approximately 15 grams. The tension on the yarn then drops to 8.3 grams, the weight of the lower jaw assembly. The electromagnetic clamps then close and there is another short time lag before the tension in the yarn begins to increase on the upstroke of the oscillating movement. The two time lags are caused by the finite length of time required for the hard rubber jaws of the electromagnetic clamp to contact and grip the brass section of the lower jaw assembly. It is to be noticed that the amplitude of the A.C. signal does not alter while the yarn is being extended; if this were not the case, then slippage in the clamp is occurring.

5.3. Change in Length During Cycling

From Figs.72-79, which show the increase in extension %, with number of cycles for the 4 types of material, it can be seen that in general there is a relatively large increase in length during the first 100 cycles followed by smaller increases above this value up to the breaking point.

The y-axis values corresponding to the maximum number of cycles do not represent the breaking extension values. To achieve the breaking extension values, the stroke per cent must be added to the y-axis values.

The effect of stroke length upon the number of cycles endured is naturally quite marked and the graphs suggest that at low strokes there may be a limiting value of extension which the yarn attains quickly and then maintains for lafge numbers of cycles.

Due to the vertical scales being identical comparison can be made between the rayon and synthetic yarns. However, the initial strokes are different and the only values which are directly comparable on a relative scale are the values at the 10% stroke.

Considering the results for viscose and acetate (Figs.72-75) it would seem that acetate can withstand fatigue conditions under low strains better than viscose, in that its increase in length per cycle is very much smaller. This is clearly due to the effect of over-reaching the elastic limit in the viscose material, the yield strains being 2.0% for viscose and 3.2% for acetate.

This effect is predominant at the $2\frac{1}{2}$% stroke level, still present at the 5% level, but unnoticeable at the 10% level (when the shape of the stress-strain curve far above the yield point is the dominating factor).

Increase in twist factor of the yarn causes a decrease in the extension (%) per cycle. This is to be expected since the yarn elastic recovery becomes greater as the turns per unit length in the

FIG 71

A TYPICAL RECORD CHART

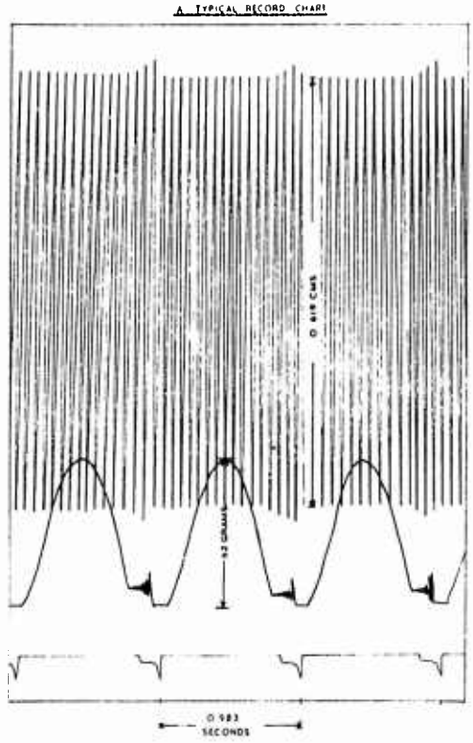

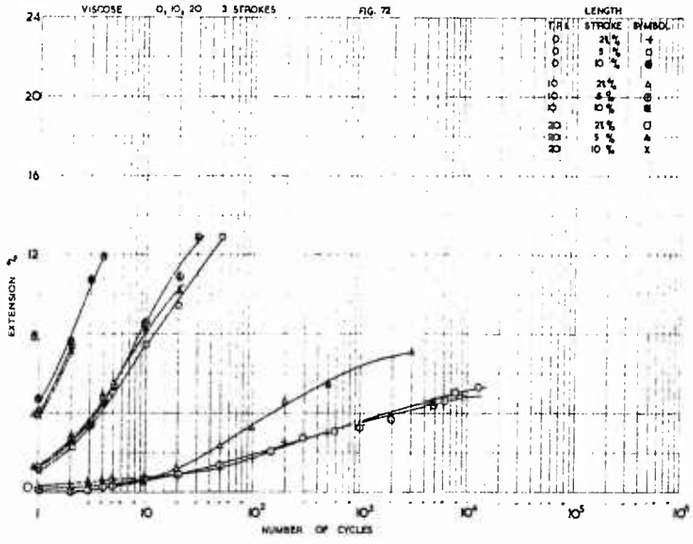

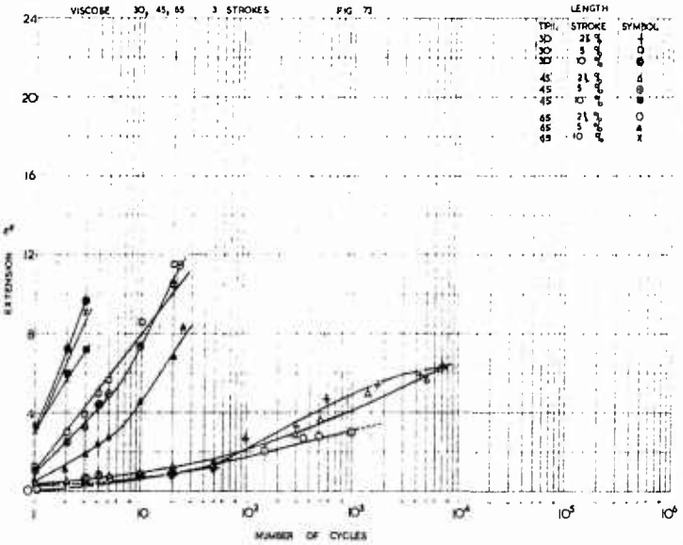

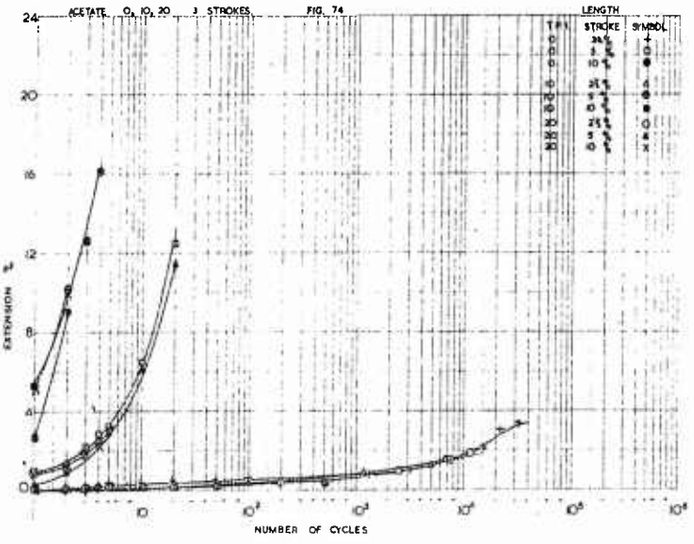

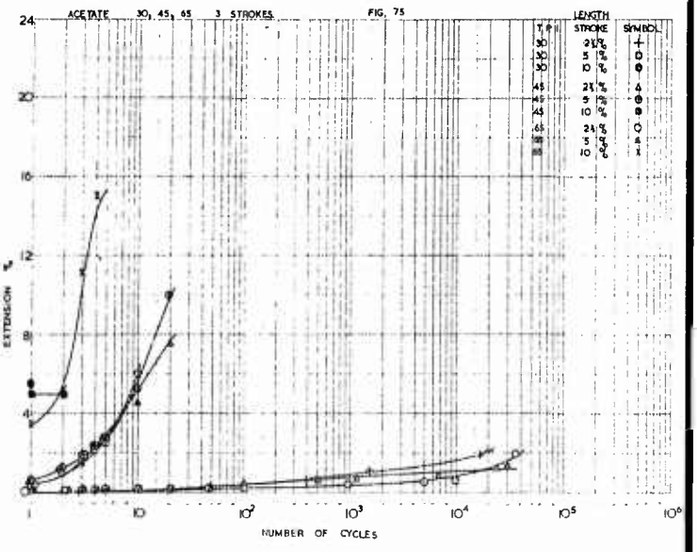

yarn is increased. This means that for a given strain, the permanent extension accruing after the first cycle is greater for a yarn with a low twist factor than for one with a high twist factor.

The effect of elastic recovery properties on the fatigue behaviour is discussed in Chapter 3.

Some difficulty arises in determining the end point of the extension-time graphs due to the distribution of number of cycles to break. It does not follow that the extension-time graph can be extrapolated beyond observed values to include those yarns which fracture at a greater number of cycles. Neither does it follow that all the specimens from a certain sample will fracture at the same breaking extension.

The procedure adopted in the graphs has been to show the curve through the observed values but extrapolation to the breaking point has not been carried out. Each curve shown represents only one specimen which, although typical, does not provide the whole picture of the fatigue behaviour for the sample.

The distribution of number of cycles to break is discussed more fully under the heading of survivor diagrams later in this chapter, but a general guide to the variability observed in extension as a function of number of cycles is that if the extension at a given number of cycles is allotted the figure of 100, then 95% of the number of observed readings will fall between figures of 75 and 125, i.e. $\pm$ 25%.

One interesting feature for the results for viscose and

acetate is that at the 2½% stroke level, i.e. when the yarns endure at least 10^4 cycles, the eventual breaking extension is much lower than at the 5% and 10% levels. The reasons for this are not fully understood, but it is very likely that severe changes in modulus, due to the repeated cycling and mechanical conditioning, take place. Due to the action of the repeated stress over long periods, the yarn will behave more and more like a glass fibre, the molecules of the structure becoming more oriented along the fibre axis. This, together with the contraction in yarn diameter and individual filament diameter, caused by extension, would account for a severe change in modulus. Another factor which no doubt affects the final breaking extension value is the amount of internal heat generated as a result of repeated cycling. Evidence to support this change in modulus is to be found in observation of samples of yarn which have broken after (say) 10^4 cycles. Although the specimen is seen to be completely broken, the lower section of the yarn remains stiff and almost vertical in the lower jaw and even after 12 hours, at least 75% of the length of the lower section of the broken specimen was observed to be vertical.

Regarding the results for nylon and Terylene shown in Figs. 76-79, the trend of development of permanent set is not dissimilar to the rayons, but the important point to note is the increase in stroke levels to produce a similar deformation for the same number of cycles.

The results for nylon at 10% stroke and for Terylene at 7½%

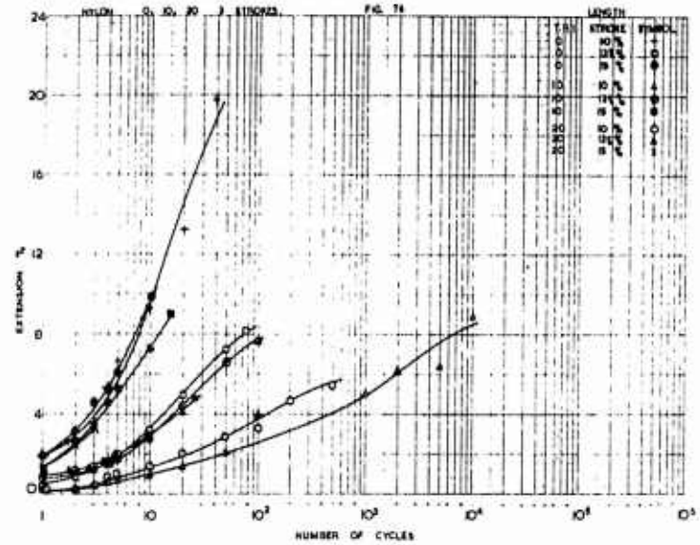
NYLON 0, 10, 20 3 STROKES.
FIG. 76
LENGTH
T.P.I.
STROKE
SYMBOL
EXTENSION %
NUMBER OF CYCLES

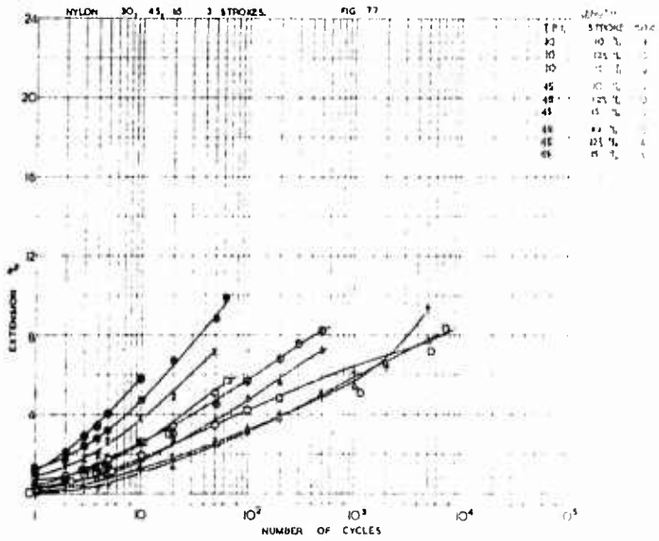
NYLON 30, 45, 65 3 STROKES.
FIG 77
EXTENSION %
NUMBER OF CYCLES

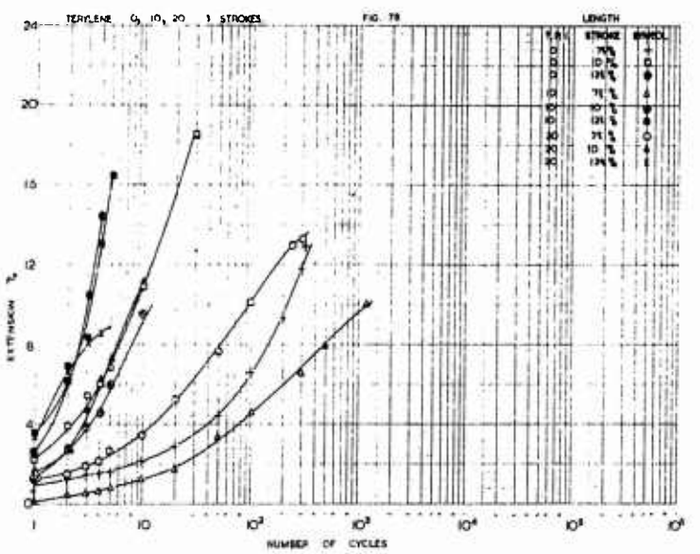
TERYLENE 0, 10, 20 3 STROKES.
FIG 78
LENGTH
T.P.I.
STROKE
SYMBOL
EXTENSION %
NUMBER OF CYCLES

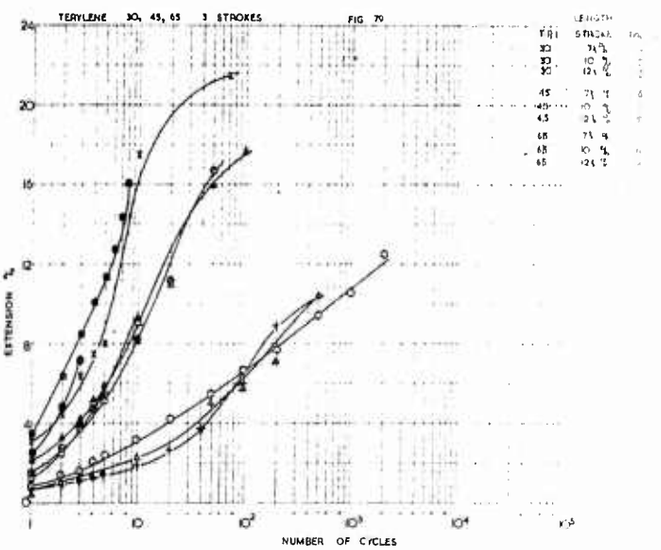
TERYLENE 30, 45, 65 3 STROKES.
FIG 79
EXTENSION %
NUMBER OF CYCLES

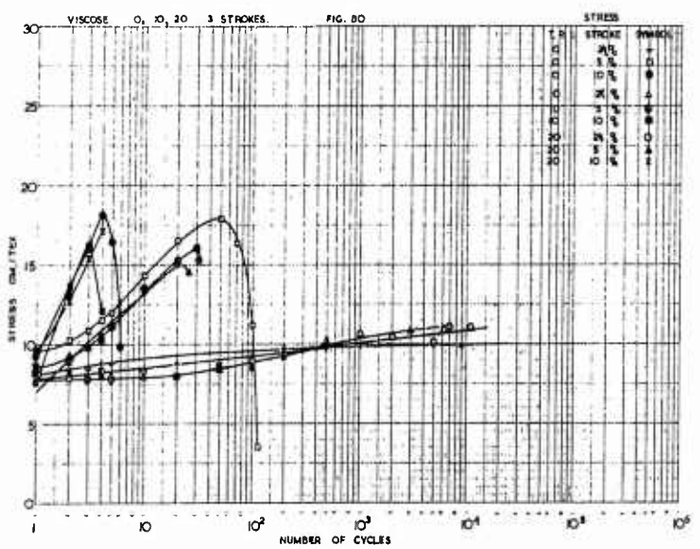
VISCOSE 0, 10, 20 3 STROKES.
FIG. 80
STRESS
T.P.I.
STROKE
SYMBOL
STRESS GM./TEX
NUMBER OF CYCLES

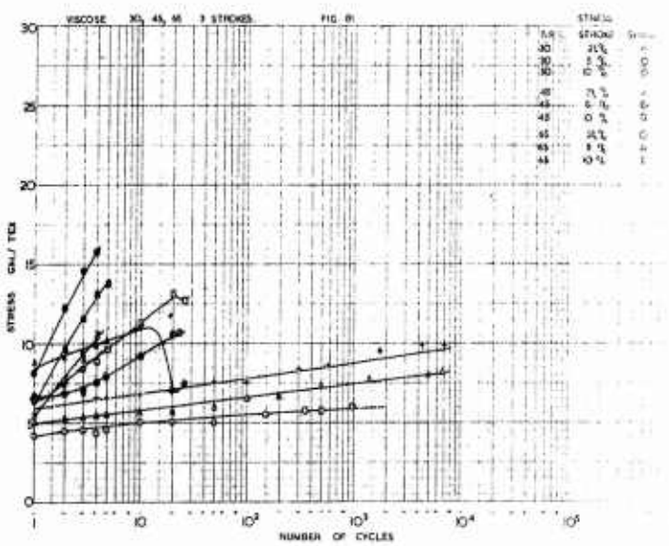
VISCOSE 30, 45, 65 3 STROKES.
FIG. 81
STRESS
STRESS GM./TEX
NUMBER OF CYCLES

stroke appear to be similar as regards number of cycles endured and this suggests immediately that nylon is superior to Terylene regarding fatigue resistance at strain levels above 7½%.

Once again, increase in twist in general, is seen to increase the fatigue life of the specimen, but there is an abnormality in the case of nylon 65 t.p.i., which although having a long fatigue life appears to grow in permanent set more quickly than its more lowly twisted companions. The values for extension at break are lower than the tensile (Instron) values by a multiplying factor of approximately 0.70 and this would suggest that the fatigue effect is definitely present and that the yarns are not just merely approaching the breaking extension gradually. It is, however, difficult to be dogmatic on this point due to the large spread in both sets of breaking extension values.

5.4. Change in Stress During Cycling

Measurements of the peak output from the strain gauge bridges are made concurrently with the length measurements and after using the appropriate calibration curve, values of tension are obtained at a progressive number of cycles throughout the test.

The values of specific stress (load divided by mass per unit length) are calculated by dividing the observed tensions by the tex values of the yarn. The units are then g.wt/tex; in the diagrams and in all references to the word stress, specific stress should be understood.

Figs.80-83 show the values of stress obtained for viscose

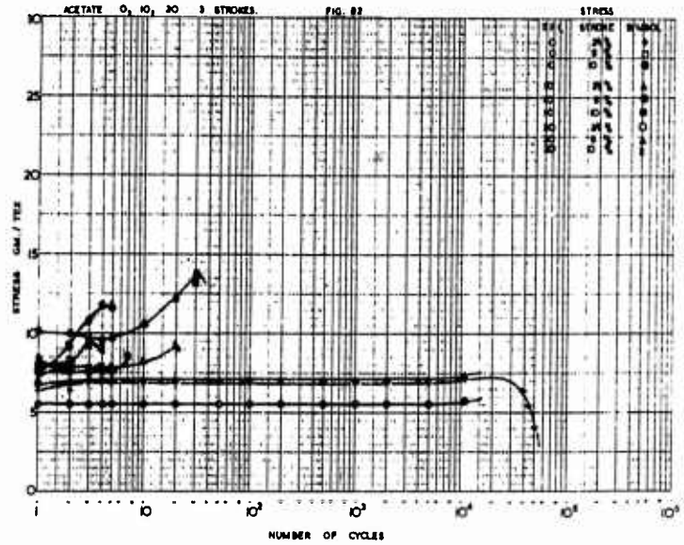
ACETATE 0, 10, 20 3 STROKES. FIG. 82
STRESS
STROKE
SYMBOL
STRESS GM / TEX
NUMBER OF CYCLES

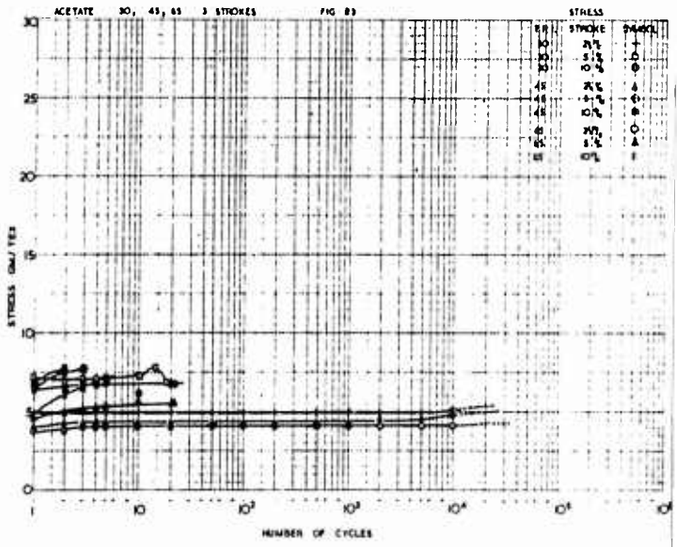
ACETATE 30, 45, 65 3 STROKES FIG 83
STRESS
STROKE
SYMBOL
STRESS GM / TEX
NUMBER OF CYCLES

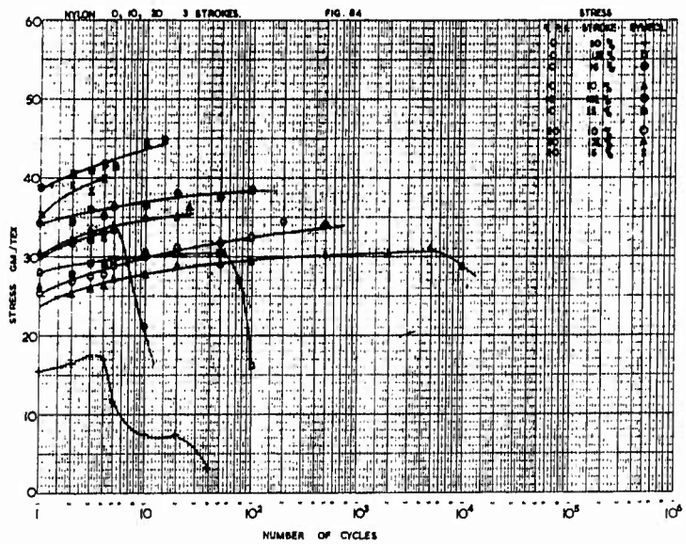
NYLON 0, 10, 20 3 STROKES. FIG. 84
STRESS
STROKE
SYMBOL
STRESS GM / TEX
NUMBER OF CYCLES

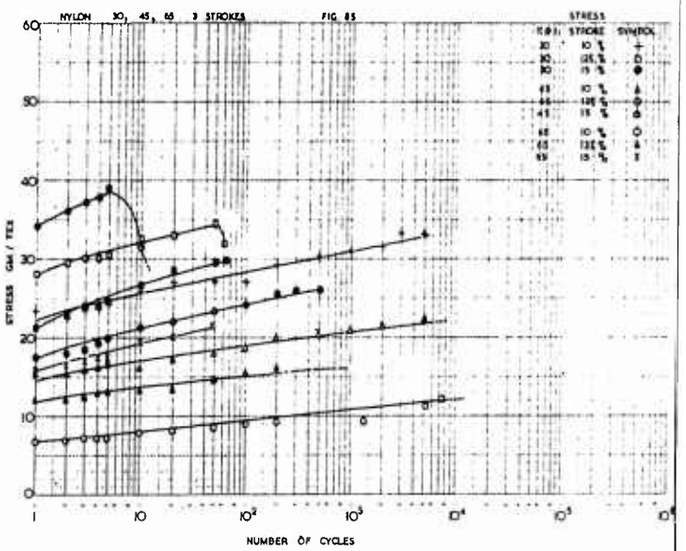
NYLON 30, 45, 65 3 STROKES FIG. 85
STRESS
STROKE
SYMBOL
STRESS GM / TEX
NUMBER OF CYCLES

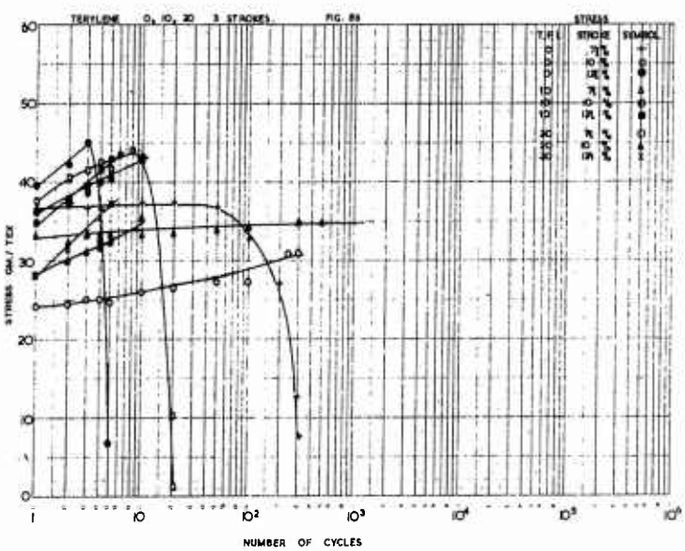
TERYLENE 0, 10, 20 3 STROKES FIG. 86
STRESS
STROKE
SYMBOL
STRESS GM / TEX
NUMBER OF CYCLES

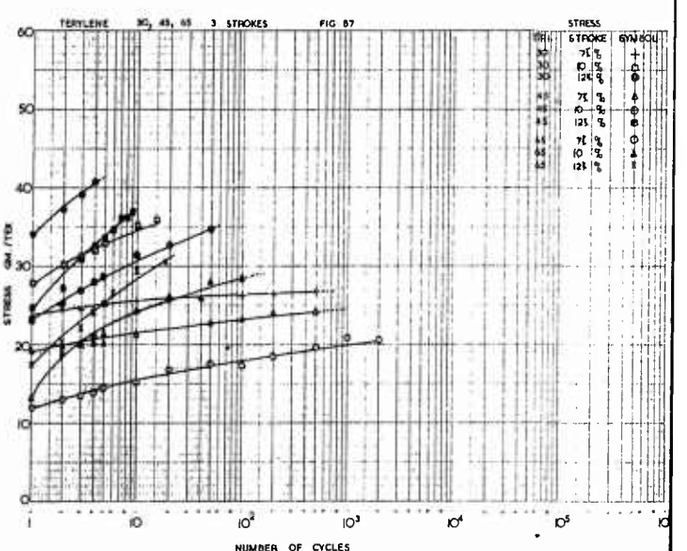
TERYLENE 30, 45, 65 3 STROKES FIG 87
STRESS
STROKE
SYMBOL
STRESS GM / TEX
NUMBER OF CYCLES

and acetate yarns at three stroke levels and for 6 values of twist factor.

It is significant that the increase in stress between the beginning and the peak value of a test is far more marked for highly twisted yarns than for those of lower twist factor. The increases range progressively from approximately 10% for the 0 t.p.i. sample to approximately 50% for the 65 t.p.i. sample. This is to be expected due to the different geometrical structure, the filaments in the more highly twisted yarn not having as much freedom and therefore suffering higher stresses if the structure is altered axially.

The values of stress on the first cycle are observed to decrease as the twist factor is increased. This vindicates the fact that the component of the stress in the filament in the direction of the yarn axis is smaller for a highly twisted yarn; the initial stress endured by the yarn, which is composed of the individual filaments, is therefore reduced as the twist factor is increased.

The effect of stroke level is very marked and this is a direct consequence determined by the portion of the stress-strain curve under observation.

In both the viscose and the acetate samples, the peak stress obtaining throughout the life of the specimen does not approach the tensile tenacity for that specimen and values of the peak stress are seen to be sometimes as low as 60% of the tenacity value. This fact is certainly significant and suggests, as do the results for extension, that the structural changes as a result of the mechanical

conditioning process of repeated cycling are very apparent and subsequent modification of basic properties is a direct consequence.

Considering Figs.84-87, the results for nylon and Terylene, it is evident that, discarding the effect of stroke level, similar arguments to those expressed above for viscose and acetate regarding changes in stress during cycling, apply in this case also. One interesting feature of these results is that at the level at which the yarns break quickly (12½% stroke for Terylene, 15% stroke for nylon), the peak stress during the life exceeds the value of tenacity as given by the Instron tests. This observation appears at all twist levels. This poses the question of whether the material is being work-hardened; however, the results probably merely reflect the increased rate of extension during the test, the fatigue tests being carried out at 180 cm/min, the tensile tests at 5 cm/min.

In all the tests involving change in stress during cycling (including those for viscose and acetate), there is a peak stress which does not always correspond to the breaking stress. This phenomenon is due to the fact that filaments are breaking after the peak stress has been reached and the maximum tension in the cycle as recorded by the strain gauges will be decreased. The effect of filament breakage on the fatigue life of the specimen is not easy to analyse, chiefly because it is virtually impossible to count the number of filaments actually broken at any stage of the test; in particular for highly twisted yarns, the ends of broken filaments often hide inside the main body of the yarn.

5.5. Tensile Tests on Unbroken Specimens

At 5% stroke, neither nylon nor Terylene samples were found to break and it was decided to compare the properties of these yarns after fatiguing them to a large number of cycles with the original yarn.

Two sets of tests were performed: in the first, 8 samples of nylon 30 t.p.i. were subjected to 300,000 cycles without failure and then transferred to the Instron tester and broken. In the second test, 13 samples of Terylene 0 t.p.i. were taken to 145,732 cycles and similarly broken.

The results for these two tests and comparison with the tensile tests on the original yarn are shown in Table XXVII.

TABLE XXVII

Properties	Nylon 30 tpi		Terylene 0 tpi	
	O.T.	T.F.	O.T.	T.F.
Breaking Extn.%	22.91	20.34	18.28	10.80
Tenacity g.wt/tex	38.69	38.44	44.38	39.94
Initial Permanent Extn. %	0.00	0.93	0.00	3.90
Modulus (g.wt/tex)	240.2	218.8	1047	788.9

O.T. = Ordinary tensile break

T.F. = Tensile after fatigue

It is apparent from this table that the repeated cycling does have an effect on the basic properties of the material, particularly in the case of Terylene. The drop in modulus is not

understood and seems contrary to expectation. It is possible that nylon and Terylene do show different behaviour regarding modulus change and the observation on the increase in rigidity was made on a viscose specimen.

5.6. Number of Cycles to Breakage

As has already been mentioned in the discussion on the changes in length during cycling, the results for number of cycles to break show a wide scatter and to illustrate the spread, survivor diagrams have been drawn. In the survivor diagram, the numbers of cycles to break are arranged in ascending order and plotted successively, until no specimens remain. The actual graph appears as an uneven step-ladder so that at any given number of cycles the number of specimens surviving is readily known.

Twenty specimens per sample from each of the 4 yarns, at 6 ranges of twist and 3 stroke levels, have been used and the results appear in Figs.88-99.

It has been found inadvisable to draw a smooth curve to represent the scatter for several reasons:

(a) A smooth curve would infer that at a certain number of cycles, a fraction of a number of specimens, e.g. $19\frac{1}{2}$ exist which is clearly not feasible.

(b) If the vertical axis is represented by survivors % to take account of (a), then the curve drawn ought to be typical of the population from which the sample is drawn. As only 20 specimens have been used, this technique would be misrepresentative, because the

FIG 88 SURVIVOR DIAGRAM FOR VISCOSE 2½% STROKE

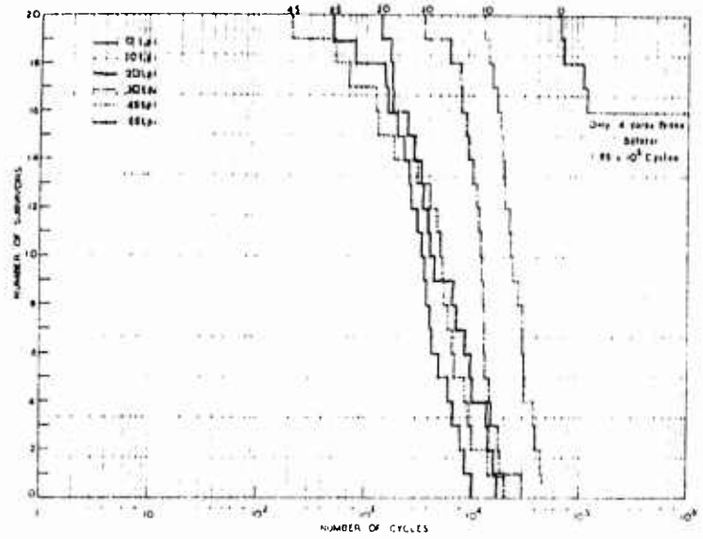

FIG 89 SURVIVOR DIAGRAM FOR VISCOSE 5% STROKE

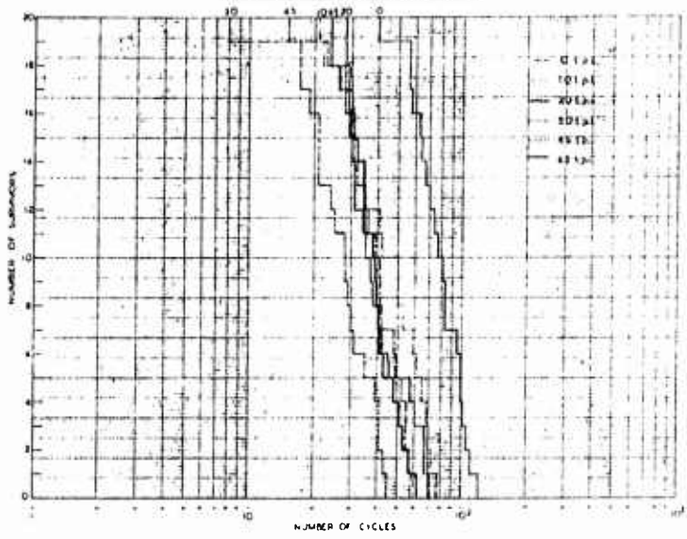

FIG 90 SURVIVOR DIAGRAM FOR VISCOSE 10% STROKE

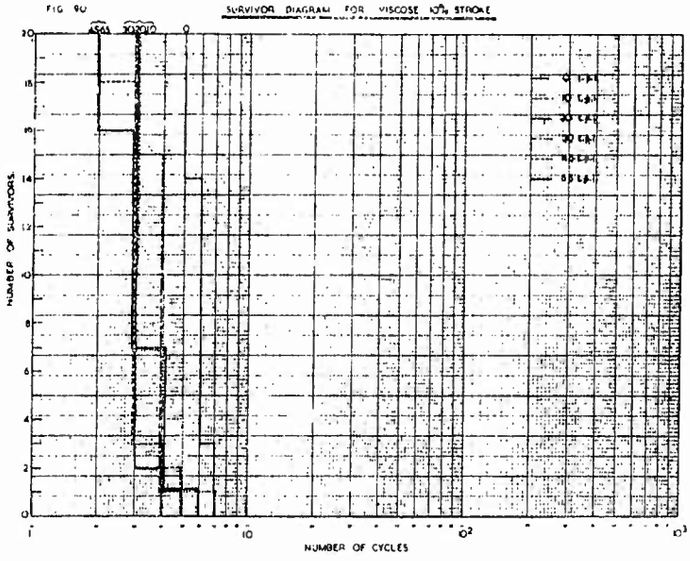

FIG 91 SURVIVOR DIAGRAM FOR ACETATE 2½% STROKE

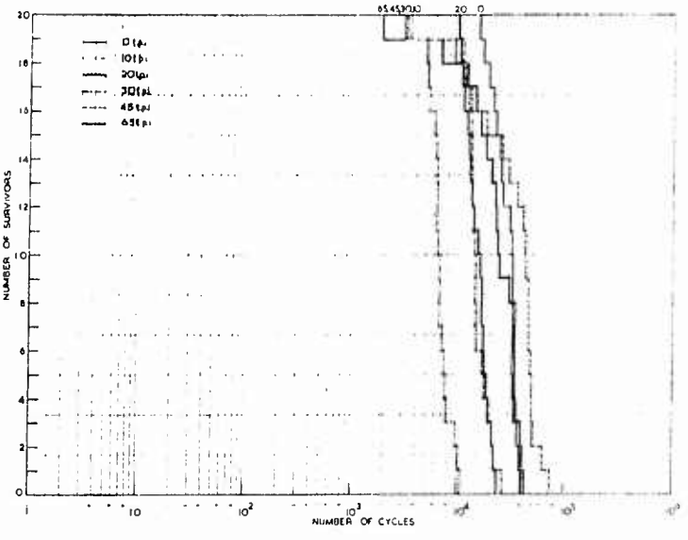

FIG 92 SURVIVOR DIAGRAM FOR ACETATE 5% STROKE

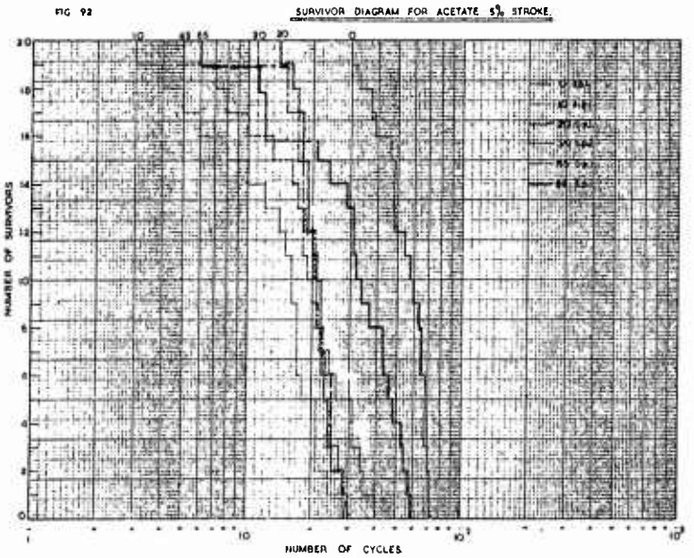

FIG 93 SURVIVOR DIAGRAM FOR ACETATE 10% STROKE

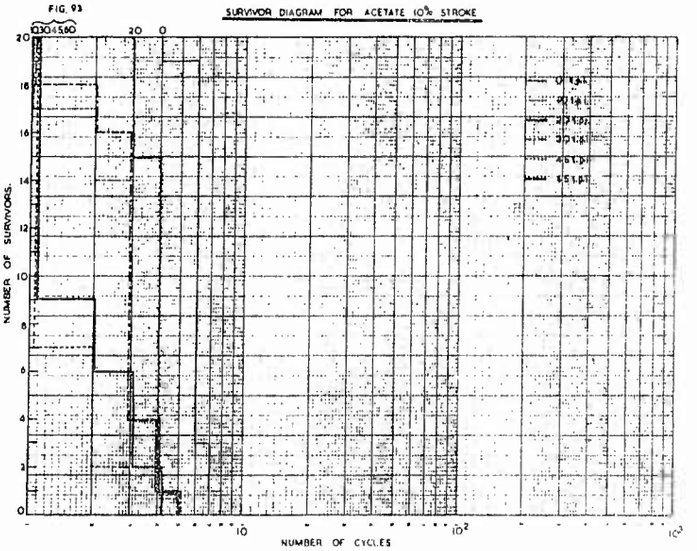

sigmoid for the population would be much flatter due to the extreme values.

(c) If a smooth curve were to be drawn, it would be difficult to decide upon the end points through which it should pass. Clearly there is a finite chance that a yarn will break upon the first cycle and it may seem reasonable to start the curve at this point. However, at the lower end of the step-ladder, where the last plotted point is on the horizontal axis, it is not correct to join the curve to this point because there is a chance that other values would be in excess of this value of number of cycles. It is not logical, however, to say that the smooth curve approaches the horizontal axis asymptotically, and will meet it at infinity, because even if an infinite number of specimens were tested, they would all break in a finite number of cycles.

In the diagrams, the effect of stroke level is seen once again to be predominant, with several yarns breaking below 10 cycles for the higher strokes. In general, an increase in the twist factor of the yarns produces more scatter, which might be expected due to the higher mean value of cycles endured for the higher twisted yarns. A more detailed examination of the statistics involved in studies of the probability of breakage due to fatigue is given in Chapter 7.

5.7. Discussion of the Results

From the results outlined above, there does seem good evidence that repeated cycling has a marked effect on the basic mechanical properties of the yarns. The picture is clouded by the

FIG 94

SURVIVOR DIAGRAM FOR NYLON 10% STROKE

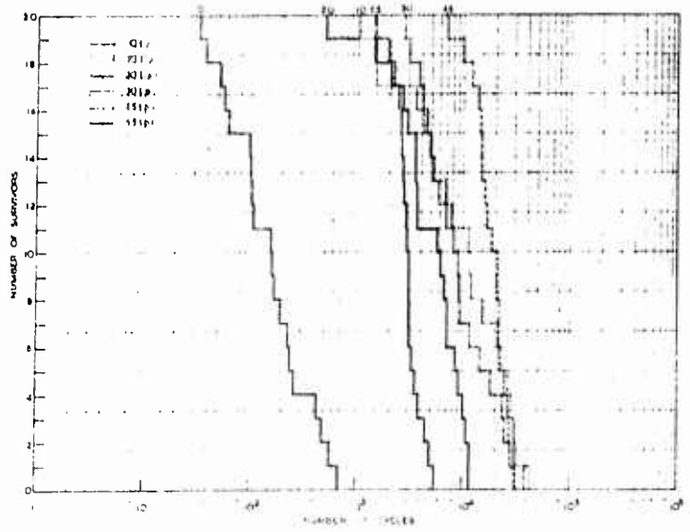

FIG 95

SURVIVOR DIAGRAM FOR NYLON 12½% STROKE

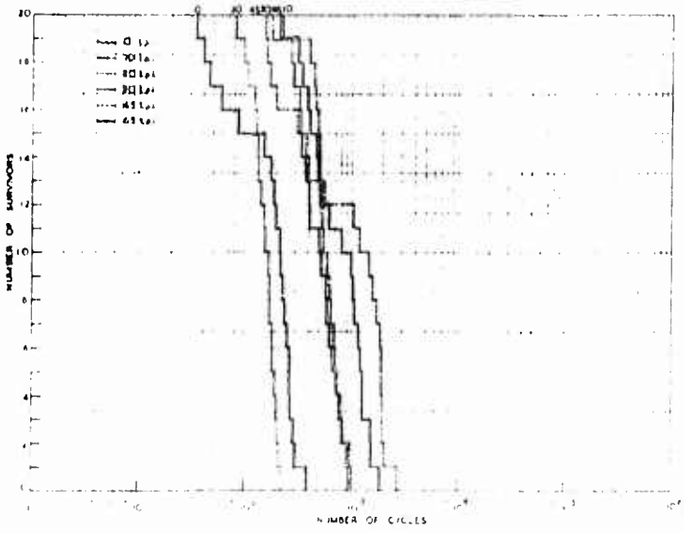

FIG 96

SURVIVOR DIAGRAM FOR NYLON 15% STROKE

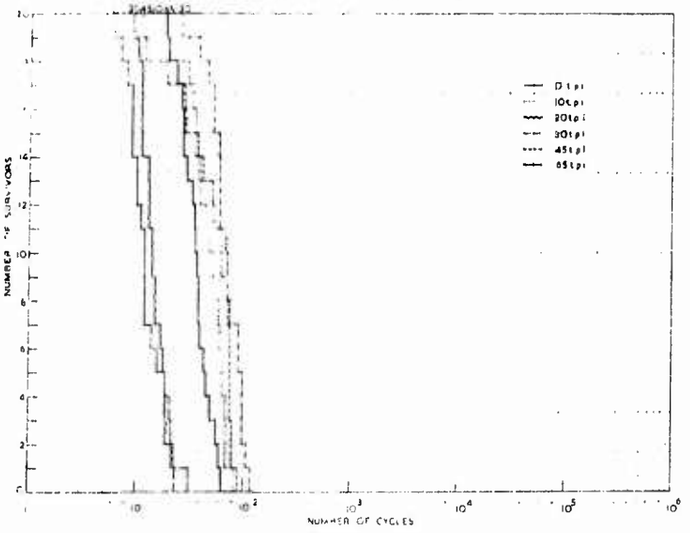

FIG 97

SURVIVOR DIAGRAM FOR TERYLENE 7½% STROKE

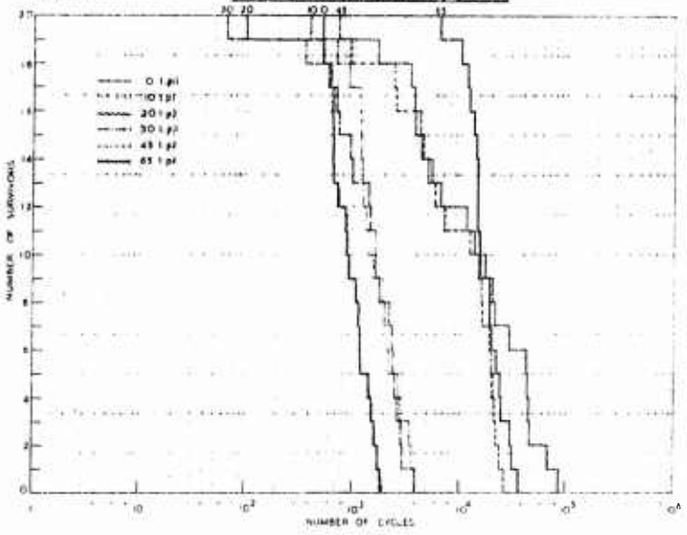

FIG 98

SURVIVOR DIAGRAM FOR TERYLENE 10% STROKE

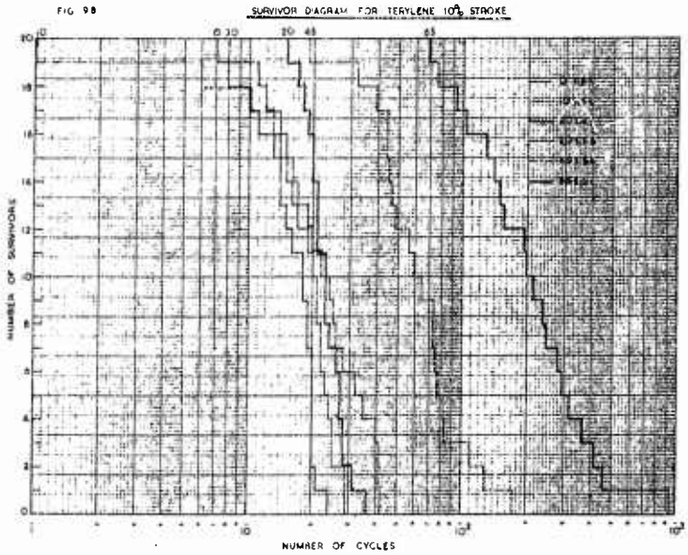

FIG 99

SURVIVOR DIAGRAM FOR TERYLENE 12½% STROKE

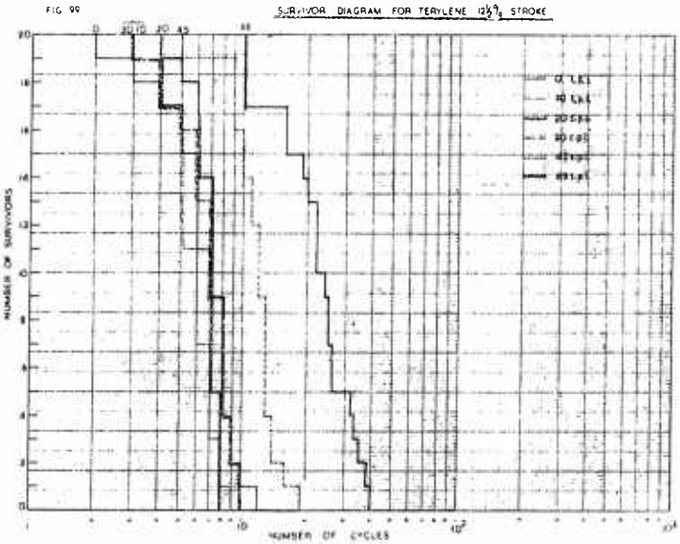

variability not only between samples but between specimens from those samples. Twist factor does appear to affect the extension and the stress developed in the yarn for all the types of material tested.

To gain further evidence of the behaviour of the yarns under fatigue conditions, a physical approach involving visual assessment of fractured filaments has been undertaken and the next chapter, Chapter 6, discusses optical techniques for use in studies on breakage and photographs showing some other aspects of the fatigue process are presented.

CHAPTER 6

PHOTOMICROGRAPHY OF FRACTURED SPECIMENS

6.1. Introduction to the Subject

The art of taking photographs showing detail of textile fibres is not an easy one to accomplish. It is very easy to produce artefacts and misrepresentations unconsciously.

Particularly in a study of fractured filaments the dangers of misinterpreting cavities, particles,cracks and surface scratches cannot be overemphasised. It is worth mentioning the merits of 5 methods of obtaining information from fibre microscopy.

1. Direct Microscope studies
2. Polarised light
3. Phase-contrast equipment
4. Interference microscopy
5. Surface microscopy, including electron microscopy.

(1) Direct Microscope Studies

This branch of study, a common one, is ideal for discovering the internal details of specimens, for example internal air bubbles, particles of delustrant, and other foreigh bodies.

By making use of reflected light as opposed to the ordinary transmitted light, other information can be gained about the nature of particles, particularly if the specimen is immersed in oil and oil immersion objectives are used. Due to a particular particle, for example, titanium dioxide in Nylon, possessing a differing refractive

index from that of its surroundings, it will reflect light and appear as a bright spot in the field of view as opposed to a cavity which will appear dark and will not reflect light.

For direct microscope work, mountants possessing refractive indices very close to those of the fibres under observation should be used. This device renders the fibres almost transparent and any inhomogeneities will be emphasised.

As is well known, many textile fibres are birefringent and possess two differing refractive indices; it is therefore advisable to choose one of these and having done so, make use of a mountant matching this refractive index.

A list of the refractive indices of the four fibres under study is given in Table XXVIII.

TABLE XXVIII

	$n_{//}$	$n_{\perp}$
Viscose	1.539	1.519
Acetate	1.476	1.470
Nylon	1.582	1.519
Terylene	1.725	1.537

For the first three fibres named, a mixture of butyl stearate (n = 1.4446) and tricresyl phosphate (n = 1.5586) can be used. For nylon, tricresyl phosphate may be used alone or otherwise cedar-wood oil, n = 1.510. For acetate fibres, it is permissible to use liquid paraffin (n = 1.470).

If a mixture is used it should be prepared according to the following formula:

$$n_m = \frac{n_1 v_1 + n_2 v_2}{v_1 + v_2}$$

where n_1, n_2 and n_m are the refractive indices of the constituents and the mixture respectively and v_1 and v_2 the volumes of the separate constituents used.

For fibres with refractive indices between 1.5586 and 1.6580, a mixture of tricresyl phosphate and monobromonaphthalene should be used. The latter named chemical has n = 1.658.

Above this range, a mixture of monobromonaphthalene and di-iodomethane (methylene iodide), n = 1.740 may be used. Terylene can be observed well in a mixture of 1 part of monobromonaphthalene and 3 parts of methylene iodide.

(2) Polarised Light

This technique is very useful for gaining information about cracks and surface markings which would not be seen in direct light or indeed with the polars at 45°. At the orthogonal or extinction position, the background is black and any surface marks or cracks appear light. It is sometimes difficult to pick out the boundary of the filament at the orthogonal position and it is possibly better from the point of view of definition of boundaries to use the polars at about 88° to each other.

(3) Phase-Contrast

Phase-contrast equipment is principally used to provide information regarding depth of cracks and the irregularities of a surface. For example with mica, the steps will appear as light bands.

(4) Interference Microscopy

The surface of fibres can be viewed quite well using a technique which employs a fibre bent into an arc; with a coverglass just touching the fibre and viewed with a double beam interferometer, Newton's rings will appear and will be distorted if inhomogeneities are present.

(5) Surface Microscopy

This process is probably the most successful and least used of all microscopic techniques. The principle is to choose a mountant having a widely different refractive index from that of the fibre and thus to throw out the surface of the fibre in deep contrast.

A mountant recommended is methylene iodide which is saturated with sulphur (n = 1.79). This is obtained from B.D.H. It can be used for all fibres and does show the surface as opposed to internal structural details.

It is preferable to use a mountant with a higher refractive index than the fibre because the depth of focus is dependent upon the refractive index and increases in proportion.

As a means of checking results, which is always preferable if possible, impression microscopy using replica techniques may be used. A useful mountant for this is a mixture of 3% polystyrene and 97% Xylol. The merits of electron microscopy, which is unsurpassed for fine detail at high magnification are not discussed in this very brief survey.

In surface microscopy it is preferable though costly to use

an objective possessing a correction collar, which is designed to correct the errors caused by the finite thickness of the cover glass.

In the present study, neither phase contrast equipment nor interference microscopy have been employed, but liberal use has been made of the other techniques outlined above.

6.2. Apparatus

The Watson service microscope fitted with 4 mm, 8 mm and 16 mm objectives has been used throughout the experiments. An additional objective (X97) has been used occasionally.

The microscope was used in conjunction with its eyepiece camera ($X\frac{1}{2}$) which holds quarter plates.

To ensure that the optical centres of the microscope are aligned and that Köhler illumination is present, the following steps were taken:

(1) Ensure that the lamp filament and the centre of the field condenser are in a horizontal plane.

(2) Adjust the relative heights of the lamp and the centre of the microscope mirror by suitable inserts beneath the supports until the light from the lamp filament is at the optical centre of the microscope mirror. The mirror should then be tilted to 45° to the horizontal.

(3) By sliding the lamp housing along its adjustment bars, a position will be found at which the image of the lamp filament (in this case rectangular) is sharp on the leaves of the substage diaphragm. Lock the lamp position at this point.

(4) Close the field diaphragm to a minimum and close the substage

iris to a point near to its minimum.

(5) By having a pin hole in the position of the eyepiece, it is possible to reach a position where the 3 pin holes, viz. field diaphragm, iris substage diaphragm and eyepiece, are in optical alignment. If this is not found to be true, the adjustment screws for centering the substage condenser should be used until there is no alteration in the intensity of the light through the 3 pinholes for vertical movements of either the substage condenser or the microscope drawtube. The microscope and lamp are now optically aligned.

(6) Open the field diaphragm slightlyand observe that the centre of the image remains central when the substage condenser is moved vertically.

(7) Place a specimen on the stage of the microscope, and bring it into focus for the objective to be used. Rack up the condenser until the image of the field diaphragm is in the plane of the specimen and both are in sharp focus.

(8) Open the field diaphragm until the image fills or is slightly in excess of the area of theobjective aperture. Open the substage iris until the required intensity of light is found. The field of view is now evenly illuminated.

(9) The lamp and the microscope should be firmly attached to the bench so that relative movement is rendered impossible, otherwise the above procedure will have to be repeated for each setting-up of the microscope.

6.3. Mounting of the Specimens

At the close of a fatigue test, after each yarn had fractured, samples of the broken specimens were taken from the jaws and mounted on microscope slides. Cleanliness of both the slide and the cover glass were found to be essential. Care was taken to avoid air pockets in the mountant by ensuring that the cover glass was lowered on to the specimen as slowly as possible; the film of mountant should be as thin as possible.

In the early stages of the work, liquid paraffin ($n = 1.470$) was used as the mountant, but in subsequent work, it was found that monobromonaphthalene and di-iodo-methane proved to be more useful mountants to provide information about surface effects.

In all, 170 slides were prepared. When the use of di-iodo methane was made, the information from microscopic observation had to be gained rapidly and photomicrographs taken within 2 hours of mounting, because of the evaporation of the mountant. Although sealing the slide by means of cellotape was tried, it was found to be only partially successful. A possible improvement would be to seal the slide by means of wax.

6.4. Results

Six samples of observations from each of the 4 types of yarn are shown in Figs. 100-103. In each set of 6 samples it has been endeavoured to show a typical view of the end of a broken yarn, any surface faults or inhomogeneities, and a fatigue break. As can be seen, much of the work has involved the use of polarised light and

FIG. 100

PHOTOMICROGRAPHS OF FATIGUED FILAMENTS.

VISCOSE

A X90

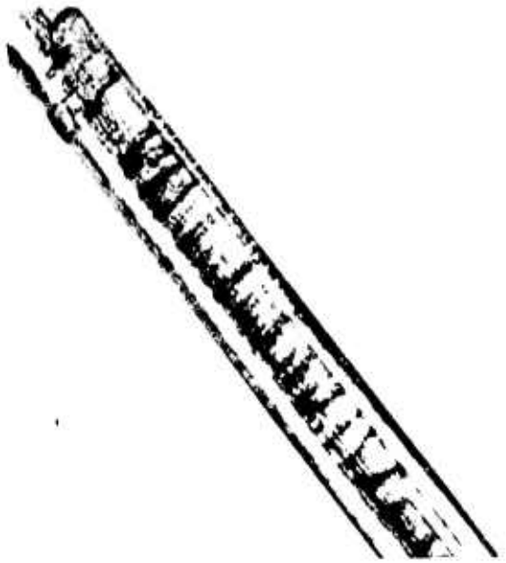

B X600

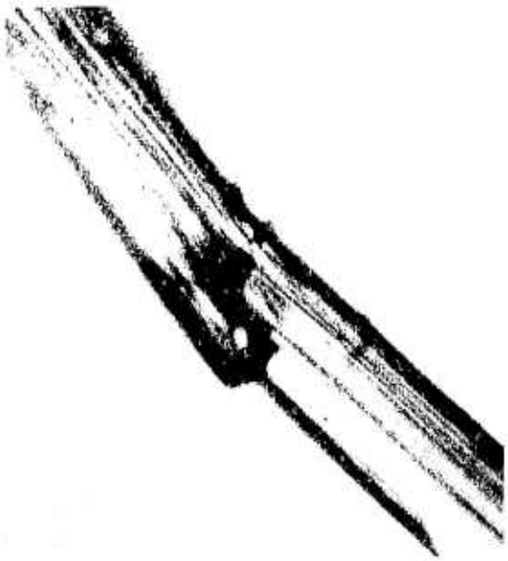

C X700

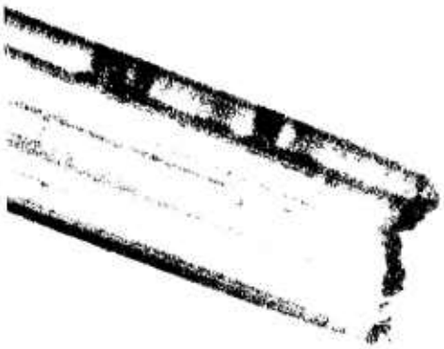

D X1100

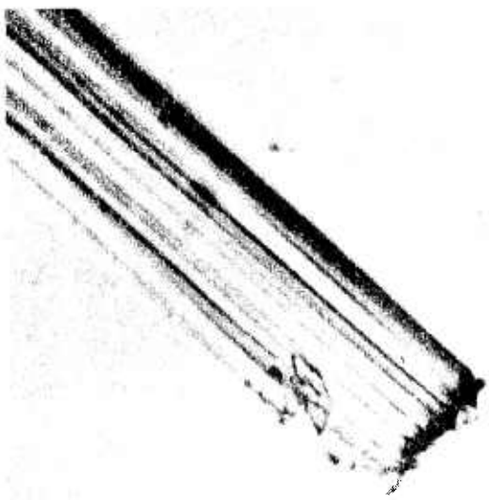

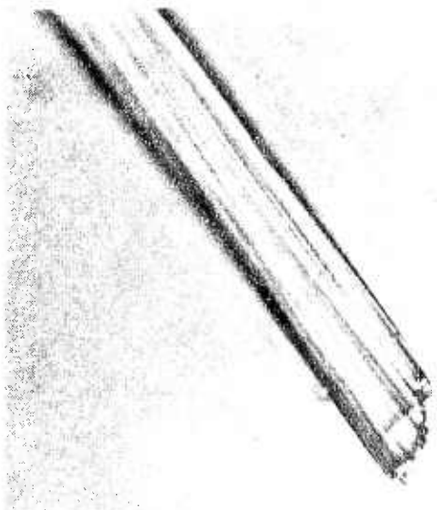

FIG. 101

PHOTOMICROGRAPHS OF FATIGUED FILAMENTS.

ACETATE.

A X 80

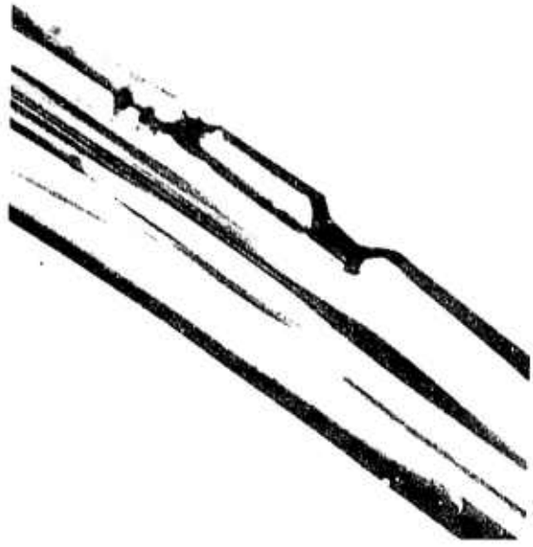

B X1000

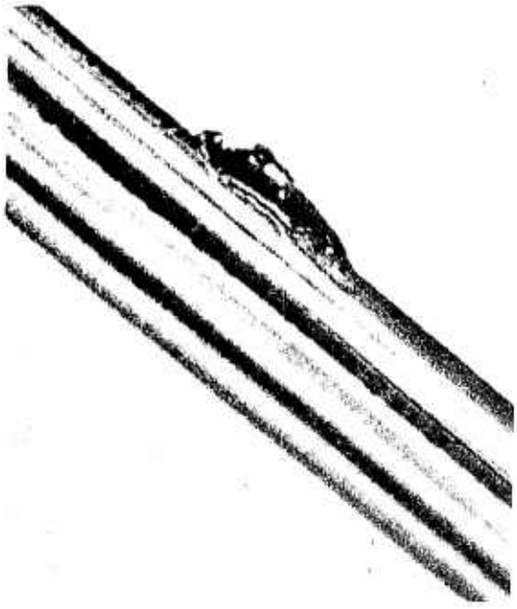

C X1000

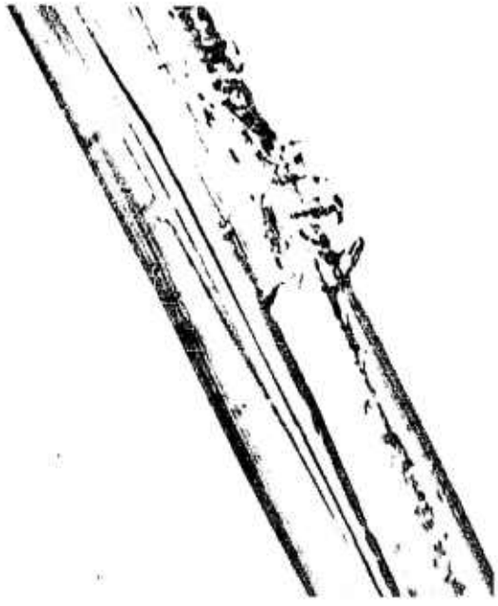

D X1000

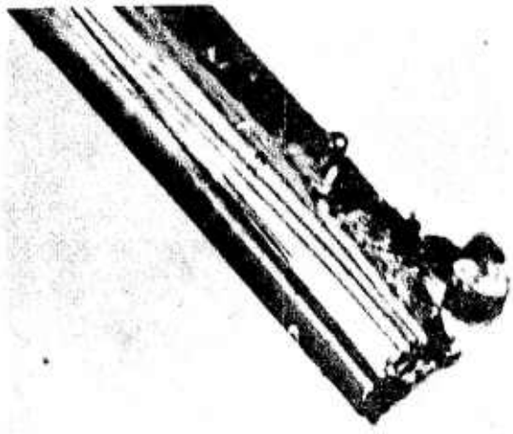

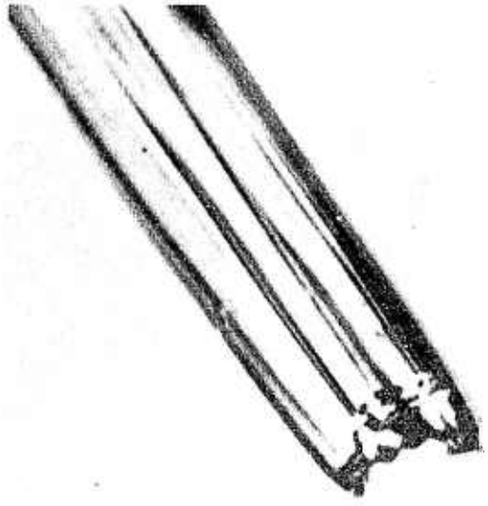

FIG. 102

PHOTOMICROGRAPHS OF FATIGUED FILAMENTS

NYLON

A X 100

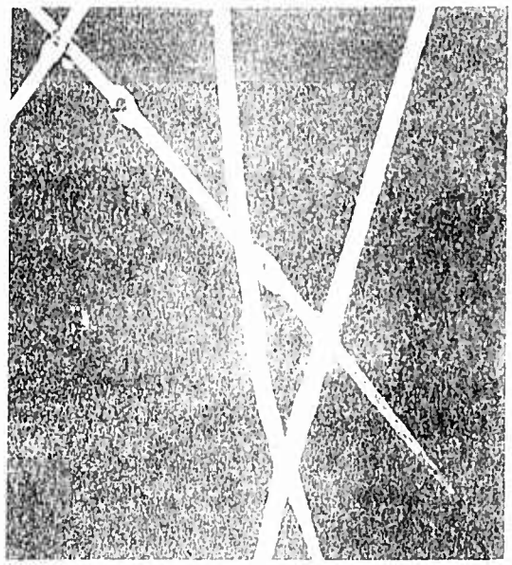

B X100

C X1100

D X150

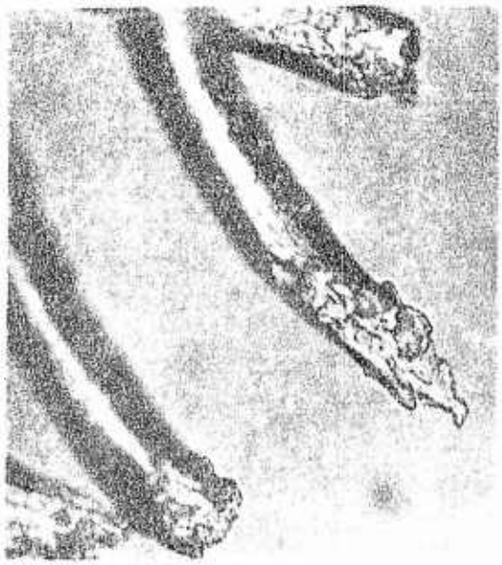

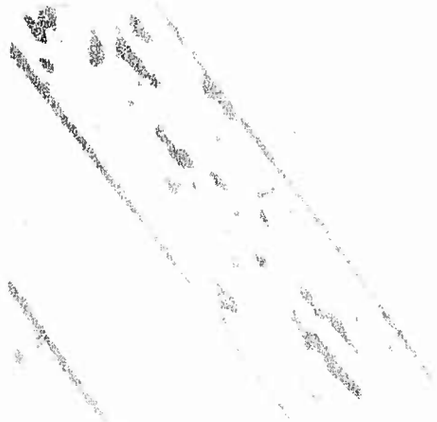

FIG. 103

PHOTOMICROGRAPHS OF FATIGUED FILAMENTS.

TERYLENE

A X150

B X900

C X1000

D X800

E X800

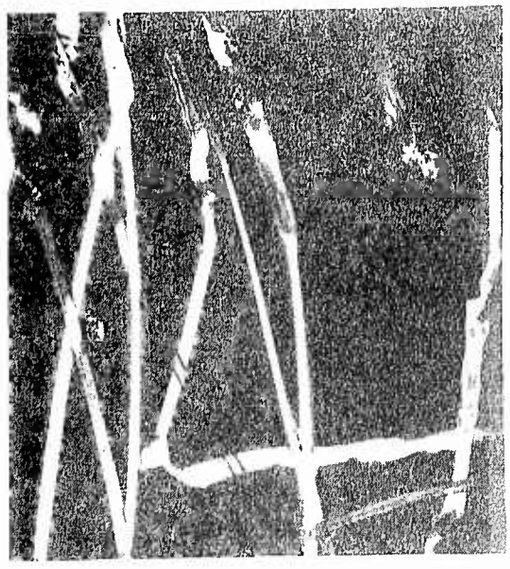

F X150

FIG. 104

DEFECTS IN NYLON

A X1000

B

C X1000

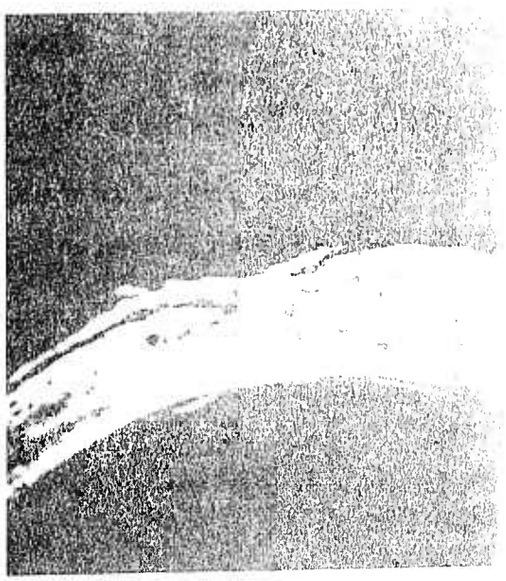

D

E X2000

FIG. 105

NYLON DEFECTS AND FATIGUE BREAKS.

A X 500

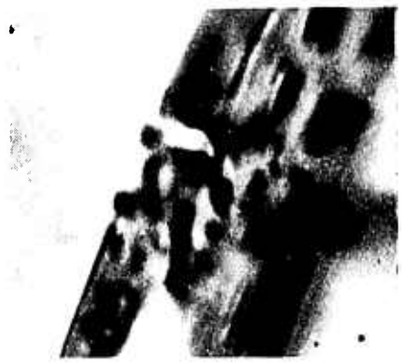

B X 1300

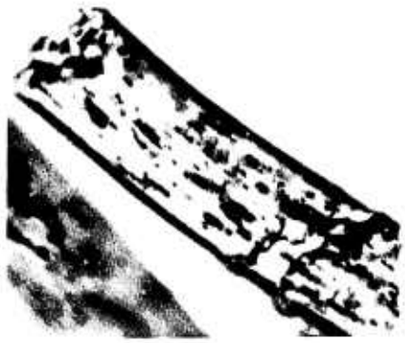

C X400

D X1200

E X1400

F X1000

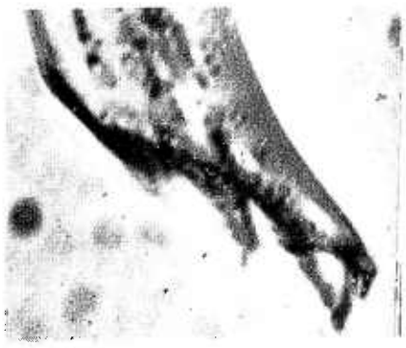

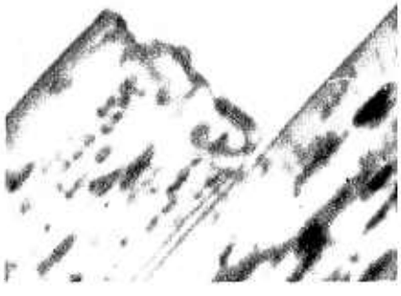

elucidation of cracks is thereby greatly facilitated.

Considering the viscose samples of Fig. 100, it is apparent that in general the fatigue breaks occurring show a fracture which is to all intents and purposes perpendicular to the filament axis although it is a jagged break. The striations due to the irregularity in cross-section may here play a prominent part in determining the nature of the break. The transverse markings which appear in Fig. 100B seem significant in this respect and may show evidence of a forthcoming crack.

Acetate would appear to behave in a similar manner to viscose but the evidence of surface damage which is apparent when comparison is made, shows that acetate, being a weaker fibre is more prone to damage of a type shown in Fig.101D being propagated to a fracture as in Fig. 101E.

In the nylon samples the appearance of the fatigue break is very markedly different to that of the rayons. As can be seen by a close examination of Fig. 102A, the majority of breaks are irregular and distorted in appearance, a typical example of which is shown in Fig.102E. A special study on nylon is made later in this Chapter, and more remarks concerning Fig.102 will be considered there.

Fig.102D which shows a filament almost fractured is interesting and supplies the information that it may be possible for a partially fractured filament to withstand repeated stress without eventual breakdown. Another possible explanation is that the occurrence of this partial fracture may be the result of "snap-back", which would

occur when the filament actually broke a little further along its length.

For the Terylene specimens in Fig. 103 , although the breaks are still not uniform, they are certainly not as irregularly shaped as in nylon. In the Terylene samples, there does seem to be good evidence for the existence of markings (Fig. 103E) and of cracks (Fig. 103D) at 45° to the filament axis. A similar partially fractured filament to that of nylon is shown in Fig. 103F.

A list of the yarns from which the photomicrographs were taken is given in Table XXIX . It would appear that twist does not have any effect on the nature of the filament break.

It was decided to investigate the fatigue fractures in nylon rather more fully due to their unusual characteristics and the fractures in Figs. 104 and 105 show some of the results found.

In Fig. 104A , the lateral displacement of the axis of the filament could possibly be due to the intertwining of filaments during stressing and as shown in Fig. 102B , at or near the cross-over points, this feature is pronounced.

Fig. 104B shows the same view this time using polarised light and from this print it would appear that a serious shearing effect has taken place. In the microscope itself the colours of polarisation are present and the colour fringes do show the shear effect quite well.

Fig. 104C shows a crack in the surface of the material and Fig. 104D brings out the damage which is present following surface abrasion.

TABLE XXIX

		T.P.I.	N	S	Mountant	Light
Fig. 100						
Viscose	A	30	904	$2\frac{1}{2}$	M.I.	0
	B	0	1.7×10^5	$2\frac{1}{2}$	M.I.	0
	C	30	904	$2\frac{1}{2}$	M.I.	0
	D	20	2199	$2\frac{1}{2}$	M.I.	0
	E	20	2199	$2\frac{1}{2}$	M.I.	0
	F	30	904	$2\frac{1}{2}$	M.I.	0
Fig. 101						
Acetate	A	30	12661	$2\frac{1}{2}$	M.I.	0
	B	20	17529	$2\frac{1}{2}$	M.I.	0
	C	0	16824	$2\frac{1}{2}$	M.I.	0
	D	30	12661	$2\frac{1}{2}$	M.I.	0
	E	30	12661	$2\frac{1}{2}$	M.I.	0
	F	20	17529	$2\frac{1}{2}$	M.I.	0
Fig. 102						
Nylon	A	0	574	10	L.P.	0
	B	0	574	10	L.P.	P
	C	65	18661	10	L.P.	0
	D	0	574	10	L.P.	0
	E	65	4.6×10^5	10	B.N.	0
	F	20	3018	10	L.P.	0
Fig. 103						
Terylene	A	30	3024	$7\frac{1}{2}$	B.N.	0
	B	30	1453	$7\frac{1}{2}$	B.N.	0
	C	20	1837	$7\frac{1}{2}$	B.N.	P
	D	20	1837	$7\frac{1}{2}$	B.N.	P
	E	30	1453	$7\frac{1}{2}$	B.N.	P
	F	10	2147	$7\frac{1}{2}$	B.N.	P

T.P.I. = turns per inch

N = number of cycles to break

S = stroke %

0 = ordinary light

P = polarised light

M.I. = Methylene iodide

L.P. = Liquid paraffin

B.N. = Monobromonaphthalene

Figs. 104E and 104F show a transverse zigzag crack. Various interpretations of the occurrence of this crack can be made but it seems feasible that progressive shearing at 45° to the filament axis has taken place. These prints are from the same crack as that shown in Fig. 103C , but are taken from a position approximately perpendicular to the latter. The first plate (102C) was taken early in the work and on later re-examination the view had altered due presumably to the moving of the filament in the mountant (liquid paraffin).

Fig. 105 shows some of the interesting phenomena encountered in fractured nylon specimens.

A. shows another quite pronounced shearing effect

B. a surface crack in the initial stages

C. a jagged break accompanied by another transverse crack, possibly caused by "snap-back".

D. an unusual three pronged break

E. an enlarged view of the crack in Fig. 102C.

F. a sheared fatigue break

G. another sheared fatigue break

H. a tensile break (Instron tester)

The parameters of testing for the prints of Figs. 104 and 105 are listed in Table XXX.

From the study of nylon it would seem possible that fatigue fractures originate from small cracks which in turn occur as a result of shearing effects and it is interesting to try to form a picture of the underlying fatigue mechanism at work.

TABLE XXX

(all Nylon specimens)

	T.P.I.	N	S	Mountant	Light
Fig. 104					
A	0	574	10	L.P.	0
B	0	574	10	L.P.	P
C	65	18661	10	L.P.	P
D	65	18661	10	L.P.	0
E	65	18661	10	L.P.	0
F	65	18661	10	L.P.	P
Fig 105					
A	65	87566	10	L.P.	0
B	65	18661	10	L.P.	0
C	65	18661	10	L.P.	0
D	65	18661	10	L.P.	0
E	65	18661	10	L.P.	0
F	65	34825	10	L.P.	0
G	65	34825	10	L.P.	0
H	65	Tensile	-	L.P.	0

T.P.I. = turns per inch

N = number of cycles to fracture

S = stroke %

L.P. = liquid paraffin

0 = ordinary light

P = polarised light

6.5. Mechanism of Fatigue

While considering fatigue in textile fibres, it would be foolish to discount the many theories of fatigue in metals which have been propounded in the past.

Theories of fatigue include:

(a) Rankine's theory of maximum stress

(b) Saint-Venant's theory of maximun strain

(c) Coulomb's theory of maximum shear stress

These theories suffer from the following inadequacies:

1. Dynamic not static strain is applied and this means that the classical theory of elasticity does not necessarily hold true.

2. The calculations involved in the theories above use the differential and integral calculus which assumes continuity and homogeneity of the material.

However, physical matter is not built up of infinitely small particles but of finite quantities, as the quantum theory shows. Metals are neither continuous nor homogeneous; even those which consist of a single phase such as pure iron, are composed of unequal crystals having different orientations and shapes and in the case of steel there are always at least two phases, cementite and ferrite.

3. The theory of strength of materials assumes uniform stress distribution, whereas the concentrations of stress may attain considerable values in practice.

4. Hooke's Law, although suitable for static forces may well be no longer applicable where dynamic stresses occur, because the

removal of the stress is not always accompanied by the immediate disappearance of the strain it produced; on the contrary a certain amount of hysteresis is usually present and unless the applied stress is very small, the metal requires a certain time to return to its primitive dimensions after the stress is removed.

Other theories of fatigue postulate molecular slip, strain hardening, a limiting value of strain energy imposed or damage caused as a result of internal damping.

All solids are full of minute defects, truly ultra-microscopic inclusions and if it were possible completely to eliminate these defects from metals their strength would be increased tenfold. In fact, metals do behave better if they are prepared by processes permitting a more complete elimination of their various impurities. When the applied stresses are variable, repeated or alternating, the superposition of secondary stresses (caused by internal stresses probably due to mechanical treatments) upon the nominal applied stress takes place in a manner which it is impossible to determine beforehand. Vibrations may produce local high stresses by phenomena of interference and it is possible to believe that the resultant of these various forces may locally exceed the cohesive strength of the metal. A microscopic crack results and this is the beginning of a fatigue failure; the crack once begun spreads into the interior of the metal more or less rapidly according to the magnitude and number of the applied stress cycles.

The arguments outlined above could well be applied in the

case of polymeric materials, but the elasticity of textile fibres imposes certain limitations on the direct applicability of the theory above. A strain in a filament produces more direct structural change than a strain of similar magnitude would do in a metal. There is interesting evidence in the observed fatigue breaks in nylon, the majority of which show sheared breaks. Regarding the zig-zag crack shown in Figs. 104E and 104F, it is possible that slab shearing has occurred possibly as a result of transverse markings. W.Lüders (1860) (59) observed such markings in mild steel and copper and Taylor (1934) (60) put forward a theory for the development of such markings and subsequent propagation. More recently Zaukelies (61) has observed slip bands, in nylon 66 and 610 and interprets his observations to be Orowan kink bands, which other observers seem to think may be Lüders' bands. Orowan bands are observed in metal wires and apparently have only been found in single crystal structures. The extension of these bands to the realm of high polymers, involving polycrystalline structure is a dubious step.

The propagation of the crack in terms of crystal lattices is a study on its own and no attempt has been made in this work to produce any evidence in this direction, although future study could incorporate this.

6.6. High Speed Photography

The actual point of breakage in the fatigue test is certainly of great interest and attempts were made to photograph the yarn just as it broke.

For this a yarn specimen possessing a short relatively constant fatigue life (17 cycles) was used.

A high speed camera, Fastax WF14, maximum speed 8000 frames per second, was used and 3 100 foot films, one with Tri-X negative and two with Plus X negative films were taken.

Due to the uncertainty in the actual time of break ($\pm$ 3 secs) a speed of 600 frames per second was used.

On one film, the actual break was caught but the break itself was on one frame only. Due to the movement of the yarn, however, little was gained from the picture and as enlargement increases the grain and decreases the definition of the print, no useful information was gained and the project abandoned.

CHAPTER 7

STATISTICAL ASPECTS OF FATIGUE

7.1. Introduction

The interpretation of results of tests involving specimens subjected to repeated load or strain cycles is made difficult by the fact that progressive damage, which finally leads to fatigue failure, is a process that is essentially determined by happenings on the sub-microscopic scale; on a phenomenological scale its cumulative effect becomes visible only at such an advanced stage of the test that most of the damage would appear to have been done. Because of the structure sensitivity of such a process the results of fatigue tests show a much wider scatter than the results of any other mechanical test. The principal difficulties with regard to the interpretation of results of fatigue tests are the microscopic heterogeneous and anisotropic inelastic effects at overall stresses below as well as above the elastic limit or yield point. This influence of inelasticity as well as that of surface condition is necessarily the more pronounced the more non-homogeneous the elastic stress field. Practically all existing fatigue theories operate on the assumption that fatigue can be explained in terms of a single mechanism. The fact is not considered that one mechanism alone can hardly be expected to describe a phenomenon that is the result of force- and time-dependent processes on the microscopic and submicroscopic level, which are associated with the existence of highly localised

textural stress fields, defects and anomalies in the ideal structure of the material.

In brittle materials it is possible to base the statistical approach to fatigue on the assumption of the existence of a statistical distribution function of the separate strength of atomic or molecular bonds within a material built up of discrete particles without recurrence to the concept of micro-cracks and stress concentrations; this implies that the distribution of bond forces or of bond energies is not, like that of stress concentrations, static and invariable but rather of the nature of a continually fluctuating distribution, as waves of thermal energy pass through the material. As a result of the thermal motion of the elements, there are incessant small changes in the structure of the material close to its condition of equilibrium which may be considered as thermal density fluctuations (see Eyring et al.(64)). Since the frequency of these fluctuations is by several orders of magnitude higher than the highest frequency of applied load cycles the local structure of the material will change from one moment to another during each load cycle; thus the probability that its response to consecutive applications of the same load cycle will be the same is infinitely small. Hence instead of introducing the probability of bond separation at a particular location or of an invariable spatial distribution of bond strength, the probability is introduced of the momentary coincidence of the separation strength of an individual atomic or molecular bond with a force in this band produced by

the external load which is sufficient to overcome the momentary level of bond strength at the unspecified location at which this coincidence occurs.

In a system of analysing any set of results which shows large scatter and particularly in a fatigue test where the primary interest lies in the time to failure of specimens, the distribution of the observations is of paramount importance and if it can be ascertained accurately it can be used to predict failure.

Several workers have presented methods of dealing with the problems associated with statistics of extreme value data, possibly the most notable being Tippett (Biometrika,1925). More recently, however, Weibull (62) and Freudenthal and Gumbel (63) have presented interesting theories concerning interpretation of fatigue tests on metals and these will be suggested as a possible means of expression of the results found for twisted yarns.

Weibull has put forward a "weakest link" theory of fatigue failure and this is outlined below.

Assume that we have a chain consisting of several links. If we have found, by testing, the probability of failure P at any load x applied to a "single"link, and if we want to find the probability of failure P_n of a chain consisting of n links, we have to base our deductions upon the proposition that the chain as a whole has failed if any one of its parts has failed. Accordingly, the probability of nonfailure of the chain $(1 - P_n)$ is equal to the probability of the simultaneous non-failure of all the links. Thus we have

$(1 - P_n) = (1 - P)^n$. If then the d.f. of a single link takes the form $F(x) = 1 - e^{-\phi(x)}$ we obtain $P_n = 1 - e^{-n\phi(x)}$ which gives the appropriate mathematical expression for the principle of the weakest link in the chain, or more generally for the size effect on failures in solids.

The same method of reasoning may be applied to the large group of problems, where the occurrence of an event in any part of an object may be said to have occurred in the object as a whole, e.g. the phenomena of yield limits, static or dynamic strength, electrical insulation breakdowns, life of electric bulbs or even death of man as the probability of surviving depending on the probability of not having died from many different causes.

He also states that:

"It is believed that in cases of random variables such as strength properties of materials, the only practicable way of progressing is to choose a simple function, test it empiricially and stick to it as long as none better is found."

Any statistical theory of the fatigue failure mechanism is thus seen to be complex to deal with and to be vindicated would involve a very large number of long period tests. In the light of the tests which have been made, the results of which are presented in Chapter 5, it would seem profitable to test the fit of the observed values to certain distributions.

7.2. Possible Frequency Distributions

The first possibility to be tried is the normal distribution and using the results of a sample of 20 specimens of Nylon 10 t.p.i., the observed values are plotted to the plotting positions $P = 1 - \frac{m}{n+1}$, where n is the number of specimens and m is the i^{th} observed value, i = 1, 2.....20, the observations being graded numerically from least to greatest.

The justification for the plotting positions used is as follows:

For any frequency function, F(x), constructed from n observations of a positive statistical variate x with the distribution $f(x) = F'(x)$, the m^{th} observation $x = x_m$ has the distribution:

$$\phi_n(x_m) = \binom{n}{m} mF(x)^{m-1} \left[1 - F(x)\right]^{n-m} f(x) \qquad (1)$$

dependent on n, m and the initial distribution, f(x). To eliminate the influence of the initial distribution, the probability function $F(m) = F(x_m)$ of the m^{th} value is taken as a new variate. Then the distribution

$$h(F_m) = \binom{n}{m} mF_m^{m-1} (1 - F_m)^{n-m}$$

has the mean (distribution free) given by:

$$\bar{F}_m = \binom{n}{m} \int_0^1 F_m^{m} (1 - F_m)^{n-m} dF_m = \frac{m}{n+1}$$

This mean cumulative frequency of the m^{th} observation differs from the frequency of the mean m^{th} value $F(\bar{x}_m)$. The mean frequency of survival as applied to fatigue results is given by the complement of this figure. The mean frequency of values exceeding x_m is

$$\ell(x_m) = 1 - \bar{F}_m = 1 - (m/n + 1)$$

If the curve of probability of survival is plotted against the number of cycles (N), using linear coordinates and the plotting positions recommended above are used, the appearance of the observed values will be scattered about a theoretical, non-symmetrical sigmoidal curve and the goodness of fit of the observations will be difficult to assess.

If, however, the ordinates (the probabilities of survival) are plotted on paper scaled in such a way as to rectify the normal distribution curve, then the points are scattered about a straight line and the task of visual or analytical tests of goodness of fit is greatly eased.

If the abscissa scale is linear then it is possible to test the fit of any function of the variate, in this case N, to see if that particular function is normally distributed. This has been done for a Nylon 10 t.p.i. yarn for the three cases N, $N^{\frac{1}{2}}$ and log N and the graphs are shown in Figs.106, 107 and 108. It is clear that the values of $\sqrt{N}$ appear to be more nearly normally distributed than those of N or log N.

It has been thought by some workers that fatigue results may be distributed log-normally and so paper has also been constructed having a logarithmic scale as abscissa and probability as ordinate. The fit of the observed value of N will appear the same on this paper as that of Fig.108.

In general, however, it has been found that fatigue results

FIG 106

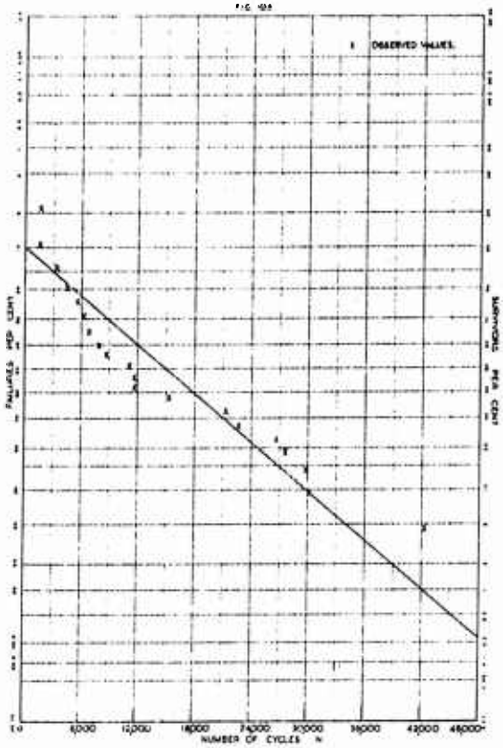

FIG 107

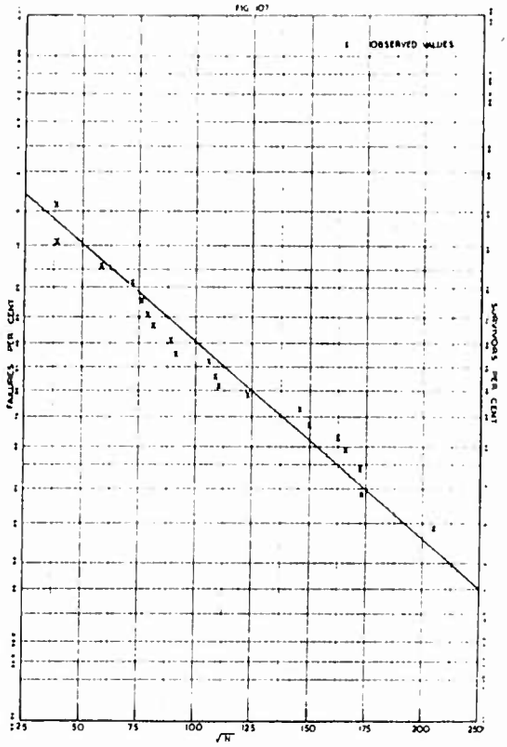

FIG 108

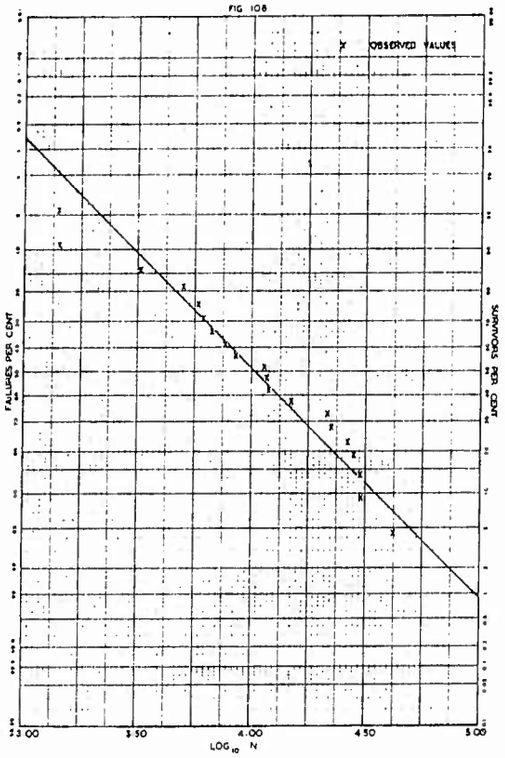

FIG 110

CUMULATIVE FREQUENCY CURVES FOR N, √N, LOG10 N

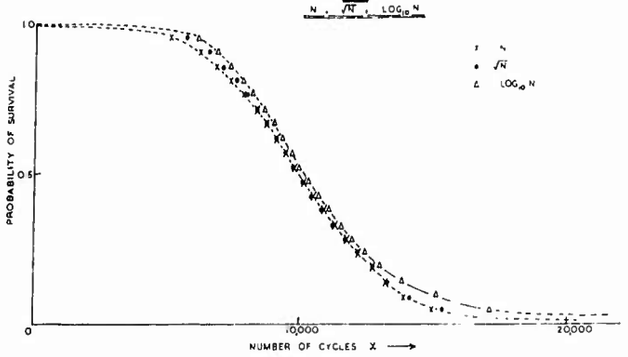

FIG 111

THE GUMBEL DISTRIBUTION

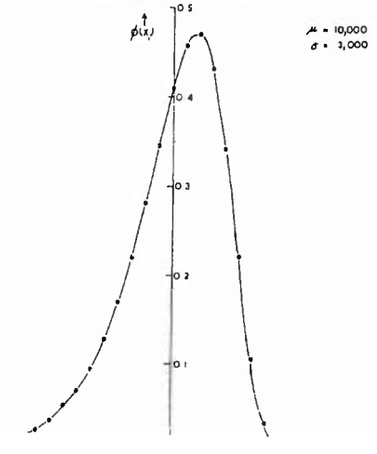

FIG 112

GUMBEL CUMULATIVE FREQUENCY DISTRIBUTION

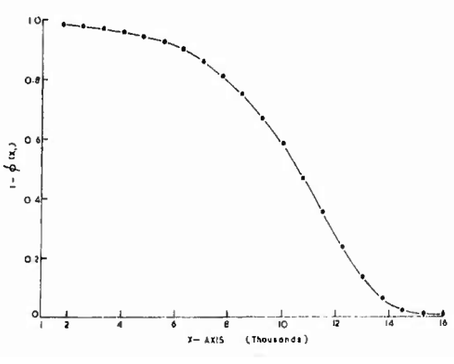

do not subscribe to a normal distribution function and it becomes necessary to look round for a distribution which will embrace extreme values more reliably. It is usual that the observed distribution of fatigue life exhibits positive skewness, i.e. the mode precedes the mean value and the curve tails off to + ∞, far more slowly than to - ∞. In this respect, there is a resemblance to the Poisson distribution but the inequality between μ and σ^2 in the observed values eliminates this completely.

The attention is now turned to distributions of the type which approach zero exponentially governed by the stipulation that

$$\lim_{x \to \infty} \frac{d}{dx} \left[\frac{1 - F(x)}{f(x)} \right] = 0$$

Amongst this type of distribution will be mentioned the Gumbel and the Weibull distributions.

When m = 1 in equation (1), the distribution of the smallest of the n values $x = x_1$ is obtained. As n increases the associated probability function tends towards the so-called "first" limiting asymptotic approximation of the form

$$^{(1)}F(x_1) = 1 - \exp\left[-e^{y}\right]$$

with a reduced variate $y = \alpha (x - u)$

α is defined by $\frac{1}{\alpha} = \frac{s\sqrt{6}}{\pi}$

where s is the sample standard deviation; u is defined by:

$$u = \overline{x_o} + \gamma/\alpha$$

where $\overline{x_o}$ is the sample arithmetic mean and γ is Euler's constant denoted by: $\lim_{n \to \infty} \left\{ 1 + \frac{1}{2} + \frac{1}{3} + \ldots\ldots \frac{1}{n} - \ell n\,(n) \right\} = 0.5772157\ldots\ldots$

The parameters of the distribution namely α and u are comparatively easy to obtain from the observed data. Both Freudenthal and Gumbel, and Weibull employ a refinement by an extension from the first to the third asymptotic approximation of the probability function of smallest values which can be made with the aid of the logarithmic transformation:

$$y = \alpha(x - u) = \ell n \left(\frac{x - \epsilon}{v - \epsilon}\right)^{\alpha}$$

where ℓn denotes the natural logarithm and v is defined by:

$$v = \bar{x} + sA(\alpha)$$

from which ϵ may be calculated by:

$$\epsilon = v - sB(\alpha)$$

In these equations, $\bar{x}$ and s are the mean and standard deviation for the observed values and $A(\alpha)$ and $B(\alpha)$ are expressions involving gamma functions, namely:

$$A(\alpha) = \left[1 - \Gamma(1 + 1./\alpha)\right] \left[\Gamma(1 + 2/\alpha) - \Gamma^2(1 + 1./\alpha)\right]^{-\frac{1}{2}}$$

and $$B(\alpha) = A(\alpha)\left[1 - \Gamma(1 + 1/\alpha)\right]^{-1}$$

Values of $A(\alpha)$ and $B(\alpha)$ have been computed by Freudenthal and Gumbel (65) for various values of the scale parameter $1/\alpha$ and corresponding skewness values ($\sqrt{\beta_1}$) denoted by:

$$\sqrt{\beta_1} = \sqrt{n(n-1)}\left\{\frac{\overline{x^3} - 3\overline{x^2}\,\bar{x} + 2\bar{x}^3}{(n-2)(\overline{x^2} - \bar{x}^2)^{3/2}}\right\}$$ are also tabulated.

For samples of 20 specimens, the above expression reduces to:

$$\sqrt{\beta_1} = \frac{\sqrt{380}}{18}\left\{\frac{\overline{x^3} - 3\overline{x^2}\,\bar{x} + 2\bar{x}^3}{(\overline{x^2} - \bar{x}^2)^{3/2}}\right\}.$$

An abbreviated table of the values computed by Freudenthal and Gumbel is shown in Table. XXXI.

TABLE XXXI

$\sqrt{\beta_1}$	$1/\alpha$	$A(\alpha)$	$B(\alpha)$
- 0.8680	0.05	0.4392	16.5744
- 0.6376	0.10	0.4250	8.7369
- 0.4357	0.15	0.4082	6.0955
- 0.2541	0.20	0.3891	4.7549
- 0.0872	0.25	0.3681	3.9326
0.0687	0.30	0.3455	3.3698
0.2167	0.35	0.3217	2.9554
0.3586	0.40	0.2969	2.6339
0.4963	0.45	0.2715	2.3755
0.6311	0.50	0.2456	2.1587
0.7640	0.55	0.2195	1.9749
0.8960	0.60	0.1933	1.8154
1.0279	0.65	0.1673	1.6748
1.1604	0.70	0.1416	1.5494
1.2941	0.75	0.1163	1.4364
1.4295	0.80	0.0915	1.3338
1.5674	0.85	0.0674	1.2399
1.7080	0.90	0.0441	1.1536
1.8521	0.95	0.0216	1.0738
2.0000	1.00	0.0000	1.0000
6.6188	2.00	- 0.2236	0.2236
19.585	3.00	- 0.1912	0.0382
60.091	4.00	- 0.1154	0.0550
190.1	5.00	- 0.0626	0.0005

It is not considered necessary to enter into the theoretical considerations which have led to the development of the two distributions outlined above, but some practical implications involved in their use will now be mentioned.

In both of the distributions, for large numbers of cycles and small probabilities of survival, a relatively small increase in the number of cycles considerably reduces the probability of survival. This phenomenon has an analogy with the popular statement concerning the last straw that breaks the camel's back.

However, in the Gumbel distribution, for high probabilities of survival, a considerable decrease in the number of cycles is necessary in order to increase the probability of survival by a small amount, whereas in the distribution associated with the third asymptotic approximation, a small decrease in the number of cycles has a large influence on the probability of survival.

One disadvantage of applying the Weibull distribution to the observed fatigue values is that occasionally the value of ϵ computed in accordance with the steps outlined above, was found to be negative due to high values of standard deviation. Freudenthal and Gumbel state that the third asymptotic approximation of the probability function of smallest values is valid only for variates bounded by $x \geqslant \epsilon$, ϵ normally being positive.

7.3. Comparison of the Distributions N, $\sqrt{N}$ and log N

Before use is made of the Gumbel distribution it is interesting to note the differences which the distributions for N, $\sqrt{N}$ and

log N exhibit.

As a means of comparison, a mean of 10,000 and a standard deviation of 3000 have been used to determine the actual curve for the $\sqrt{N}$ and log N curves.

The normal curve, constructed from the ordinates given in standard statistical tables, is used as the starting point. This curve is drawn using the multiple of standard deviation as abscissa and $\phi(x) = \frac{1}{\sqrt{2\pi}} e^{-\frac{1}{2}x^2}$ as the ordinate. The curve shows the mean, mode and median coincident at the point x = 0, when $\phi(x) = 0.3989$.

It is now desired to find values of $\sqrt{N}$ which are normally distributed and compare the distribution of the square of these values with the standard normal curve. In this way, the skewness introduced by using values of $\sqrt{N}$ instead of N will be brought out and the distribution may be found to show a better fit to observed values.

To accomplish this, equally spaced readings from the horizontal axis are taken and the mean is designated the value of 100, i.e. $\sqrt{10,000}$. Since the standard deviation for the normal distribution has been taken as 3,000, a rough first estimate of the standard deviation for the $\sqrt{N}$ distribution can be obtained by assuming that the majority of values lie between $\pm$ 1 standard deviation from the mean, in other words that:

$$(\sqrt{N}_{+1})^2 - (\sqrt{N}_{-1})^2 = 6,000$$

where $\sqrt{N}_{+1}$ and $\sqrt{N}_{-1}$ indicate the values of $\sqrt{N}$ at + σ and - σ respectively.

Since $\sqrt{N}_{+1}$ will be identical with $(\mu_{\sqrt{N}} + \sigma_{\sqrt{N}})$,

$$(\mu_{\sqrt{N}} + \sigma_{\sqrt{N}})^2 - (\mu_{\sqrt{N}} - \sigma_{\sqrt{N}})^2 = 6{,}000$$

$$\therefore \quad 4\mu_{\sqrt{N}}\ \sigma_{\sqrt{N}} = 6{,}000$$

and with $\mu_{\sqrt{N}} = 100$, this gives a rough first estimate of $\sigma_{\sqrt{N}}$ as 15.

Using this value, equally spaced readings for the $\sqrt{N}$ distribution for a mean of 100 and standard deviation of 15 are obtained.

By squaring these values and finding the mean and standard deviation of the resultant values, the frequency distribution can be plotted, providing the ordinates are adjusted to compensate for the difference in standard deviation.

The frequency of values between N and N + dN (for the normal curve) is

$$f(N)\ dN$$

where dN is a small increment of N and f(N) is the ordinate of the frequency distribution at the point N on the horizontal axis.

Similarly, if $y = \sqrt{N}$, the frequency of values in the small interval between y and y + dy:

$$= f(y)\ dy$$

For the two frequency distributions to be compared, these two frequencies of values must be equal.

$$\text{i.e.} \quad f(N)\ dN = f(y)\ dy$$

Using the identity $f(y)\ dy \equiv f(y)\ \frac{dy}{dN}\ dN$

$$f(N) = f(y)\frac{dy}{dN}$$

Now, $\frac{dy}{dN} = \frac{1}{2\sqrt{N}} = \frac{1}{2y}$

$$\therefore \quad f(N) = f(y).\frac{1}{2y} \qquad (2)^{*}$$

This equation holds for the normal curve which is calculated and drawn so that the total area under the curve, with mean of 0 and standard deviation of 1 is unity.

However, the standard deviation for the $\sqrt{N}$ curve is 15 and the ordinates of (2) therefore need to be scaled down by this factor, so that comparison can easily be made.

Having obtained these adjusted frequencies the distribution curve can be drawn.

Steps in the calculation are as follows:

(1) Tabulate $\sqrt{N}$ values, equally spaced on the horizontal axis with mean 100 and S.D.15

(2) From the normal curve, read off the ordinate values at these points.

(3) Square the $\sqrt{N}$ (=y) values to obtain values of y^2.

(4) Using the frequencies of (2), calculate the mean μ and S.D. σ for the squared values.

(5) Tabulate $(y^2 - \mu)/\sigma$

(6) Calculate the frequencies for the y values from

$$f(y^2) = f(y)\frac{1}{2\sqrt{N}} \times \frac{1}{15} \times \sigma$$

(7) Plot $f(y^2)$ against $(y^2 - \mu)/\sigma$

A similar procedure may also be used to compare the N and log N distributions. In this case, a first estimate of the standard deviation is found from the equation:

$$10^{x} - 10^{-x} = 0.6$$

This equation represents the condition that the majority of values shall lie between plus and minus one standard deviation from the mean ; x represents the value of the abscissa on a log scale at a distance of 1 standard deviation from the mean.

Solving this equation:

$$10^{x} = \frac{0.6 \pm \sqrt{0.36 + 4}}{2}$$

from which, taking the positive square root,

$$\underline{x = 0.1284}$$

The new ordinates of the frequency distribution for log N are then given by:

$$f(N) = \frac{f(z)}{0.1284} \cdot \frac{dz}{dN}$$

$$f(N) = \frac{f(z)}{0.1284} \cdot \frac{0.4343}{z}$$

the factor 0.4343 arising due to derivation.

The figure 0.1284 is introduced once again as an adjusting scale factor. The value of f(N) needs to be multiplied by the standard deviation of the log (N) values (in this case 3112) to enable plotting positions to be compared.

A graph showing the 3 graphs superimposed upon each other is shown in Fig.109.

Clearly errors are introduced by estimating the standard

FIG. 109

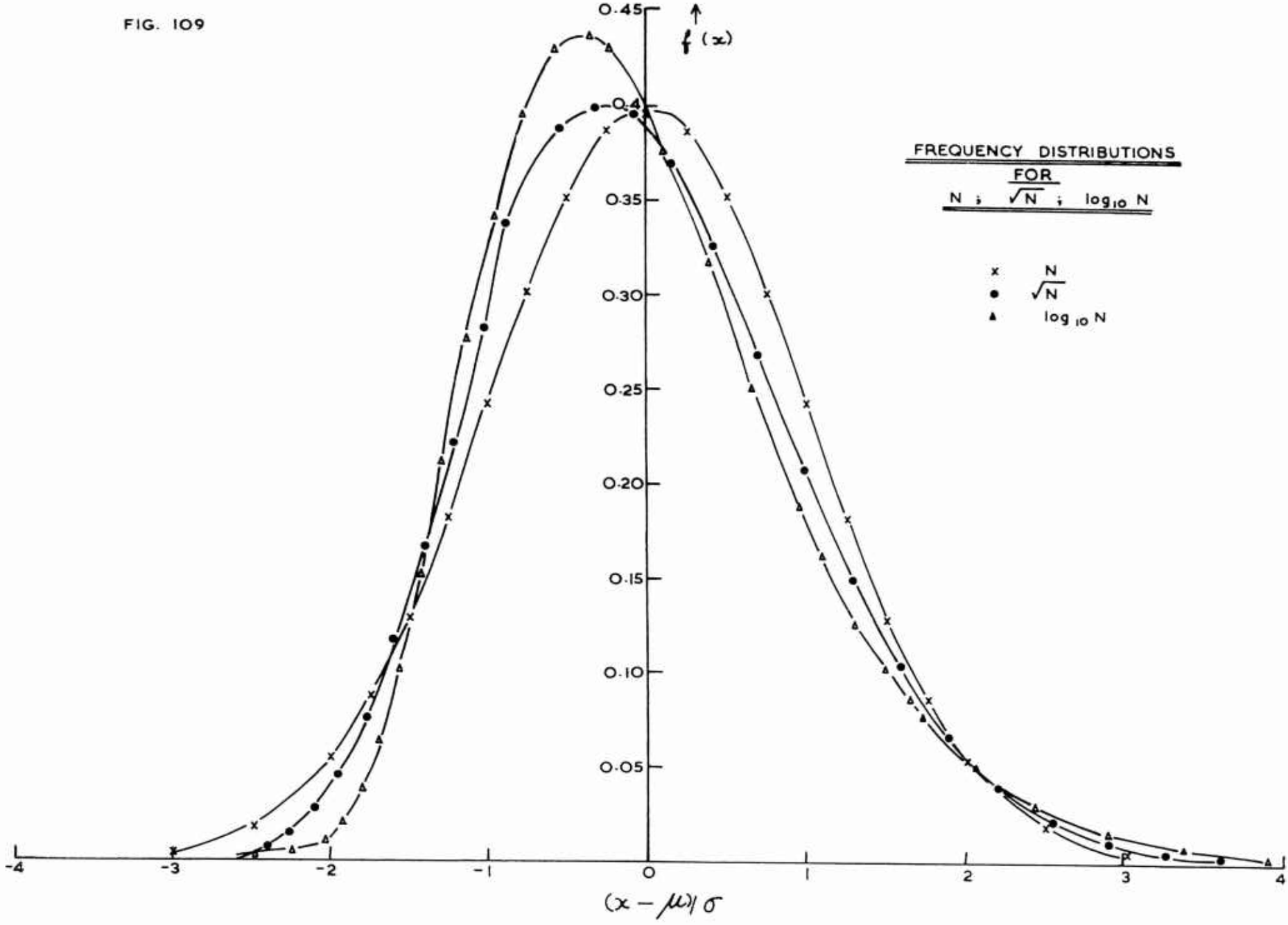
0·45
f (x)
0·4
0·35
0·30
0·25
0·20
0·15
0·10
0·05
-4
-3
-2
-1
0
1
2
3
4
(x − μ)/σ
FREQUENCY DISTRIBUTIONS
FOR
N ; √N ; log10 N
x N
● √N
▲ log10 N

deviation by the comparatively easy method outlined above and should the exact form of the curve be required, then the method of successive approximations can be applied.

The shapes of the distributions are, however, seen to be quite distinguishable and to have different features.

To obtain the cumulative frequency distributions for the N, $\sqrt{N}$ and log N curves, the area under the curve is divided into 21 equal wedge-shaped areas. This can be done either by planimeter or by counting the number of squares (the curve being drawn on millimetre graph paper). The abscissa values at which the 20 ordinate lines divide the area, are plotted against the plotting positions $P = 1 - (m/n + 1)$. The abscissa readings are converted from $(x - \mu)/\sigma$ to x, where x is the number of cycles endured and μ, σ the mean and standard deviation for the respective distributions.

The curves obtained are shown in Fig.110.

To compare the Gumbel distribution with the three distributions given above, the same mean (10,000) and the same standard deviation (3,000) were used. For the Gumbel distribution,

$\phi(x_1) = 1 - \exp(-e^y)$, the reduced variate y being given by

$$y = \alpha(x - u)$$

Here $$\alpha = \frac{\pi}{S\sqrt{6}} = \frac{\pi}{\sqrt{6}} \cdot \frac{1}{3,000} = 4.2751 \times 10^{-4}$$

and $$u = \bar{x} + \frac{0.57722}{\alpha}$$

$$= \underline{11350}$$

$$\therefore \quad \underline{y = 4.2751 \times 10^{-4} (x - 11350)}$$

For the distribution function,

$$\Phi(x_1) = \alpha \exp\left[y - e^y\right]$$

and when these values are calculated and plotted as ordinate against $(x - 10{,}000)/3{,}000$, the curve shown in Fig.111 is obtained.

The corresponding probability function

$$\phi(x_1) = 1 - \exp\left[-e^y\right]$$

can be similarly used to give the cumulative frequency distribution shown in Fig.112. In the curve shown $1 - \phi(x_1)$ is the probability of survival for the respective number of cycles.

Having chosen 4 distributions it is necessary to examine the observed data and test the goodness of fit to discover the particular distribution (if any) which is suitable.

For the N, $\sqrt{N}$ and log N distributions this has been accomplished for 3 other yarns (the results for Nylon 10 t.p.i. having already been plotted in Figs.106-108).

The yarns chosen were Nylon 45 t.p.i., Terylene 0 t.p.i. and Terylene 65 t.p.i., all tested at the 10% stroke level. The actual results are shown in Table XXXII, and the data is shown plotted against $P = 1 - \frac{m}{n+1}$ in Figs.113-121.

The lines about which the observed data fall are constructed from the known μ and σ for the particular distribution using normal probability tables. As has been mentioned earlier in this Chapter, it is easy to test the fit of the observed data due to the rectification of the normal probability curve, by the use of the arithmetical probability ordinate scale.

TABLE XXXII

Plotting Position	Nylon 45 t.p.i.	Terylene 0 t.p.i.	Terylene 65 t.p.i.
$P = 1-\frac{m}{n+1}$	CYCLES TO FAILURE		
.0476	6710	7	69
.0952	9627	8	76
.1428	11948	10	93
.1904	13701	11	104
.2380	14117	13	139
.2856	14270	14	151
.3332	14784	14	158
.3808	15957	15	163
.4284	16533	16	194
.4760	18035	18	198
.5236	20371	18	216
.5712	20426	19	236
.6188	21262	19	245
.6664	21263	20	280
.7140	22897	20	293
.7616	24893	20	319
.8096	25263	20	366
.8572	27799	20	416
.9046	28463	21	457
.9524	32424	24	919

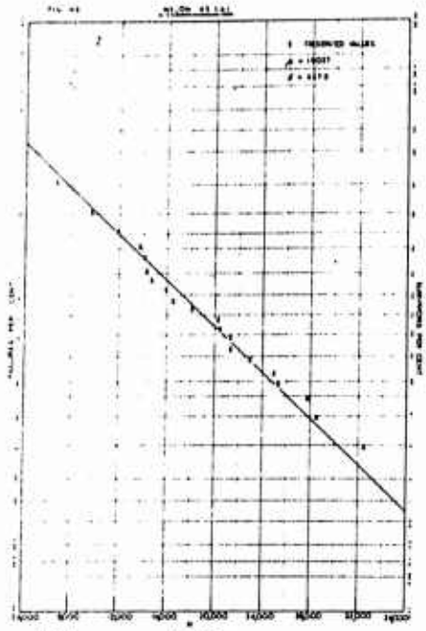

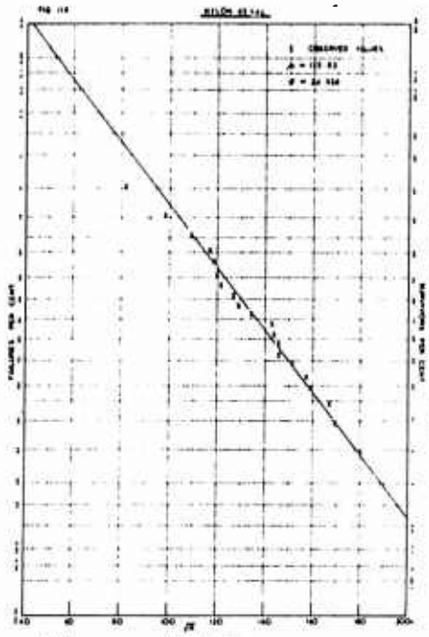

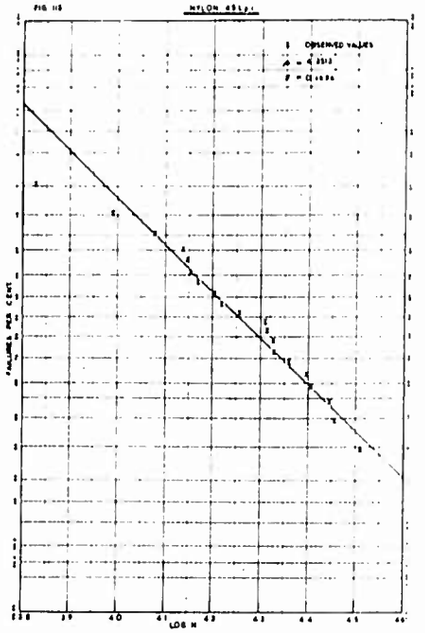

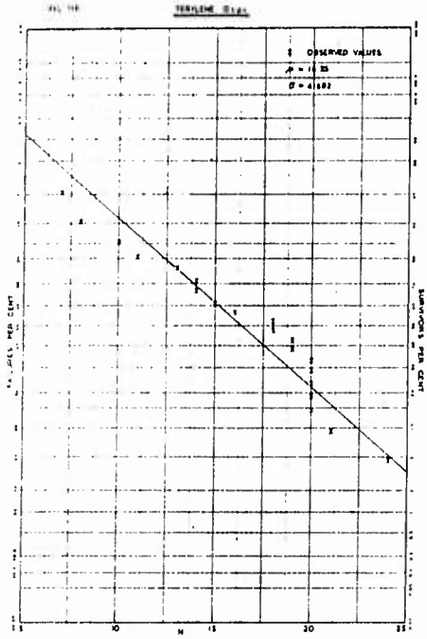

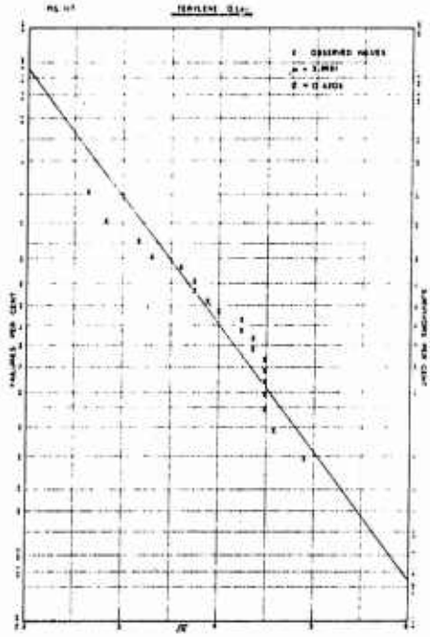

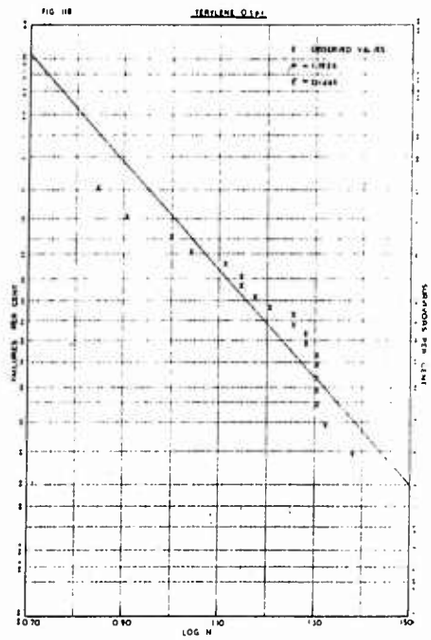

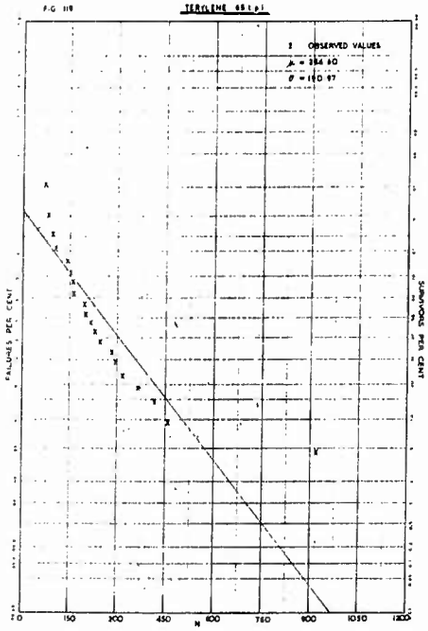

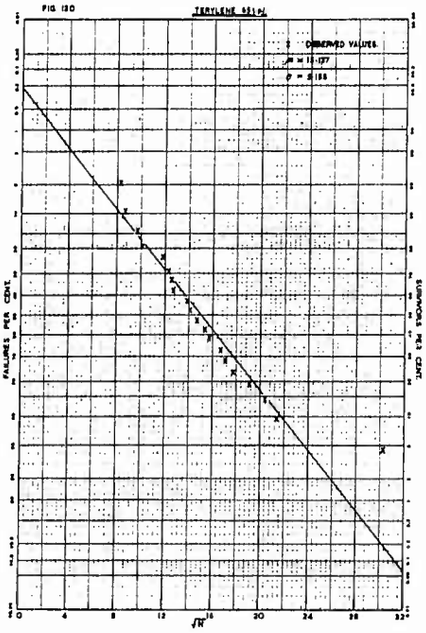

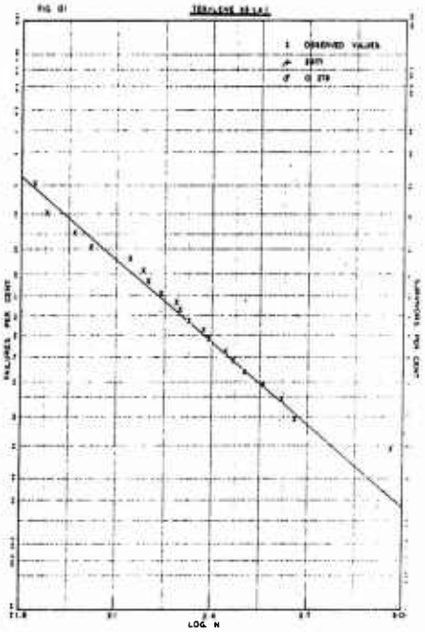

Considering the resultsfor Nylon 45 t.p.i. in Figs.113-115, it is apparent that the points are best fitted to a plot for a normal distribution of number of cycles N. When the $\sqrt{N}$ or the $\log_{10}N$ distributions are introduced then the goodness of fit is impaired. This would suggest that the number of cycles to failure are normally distributed with a mean of 19037 and a standard deviation of 6678 cycles.

For the results of Terylene 0 t.p.i. shown in Figs.116-118, it also seems that the plot against N provides the closest fit.

For Terylene 65 t.p.i., however, the fit of the data is very poor due almost entirely to the spurious point at 919 cycles. The log N distribution is the nearest to take account of this extreme value.

Several interesting points come out of the scrutiny of these graphs. Firstly, it would seem in two cases that the number of cycles to failure would appear to be normally distributed. In one of these cases, the Terylene 0 t.p.i., this consequence might be expected to be due to the low number of cycles to break which occurs. As the breaking extensions of yarns in many cases are normally distributed it could be assumed (though somewhat dangerously), that the so-called fatigue test in this case merely demonstrates a cumulative extension test, culminating in breakage at the breaking extension.

However, in contradiction to this statement, the other sample, Nylon 45 t.p.i., would not be expected to show this behaviour.

For the Nylon 10 t.p.i. (Figs.106-108), the conclusion may be drawn that $\sqrt{N}$ values are more nearly normally distributed than N or log N values. In the case of Terylene 65 t.p.i., the log N values are more nearly normally distributed, though in this latter case, bias is introduced to a considerable extent by extreme values.

A direct consequence of this last statement is that since the extreme values of N, particularly at the lower end of the scale, are of considerable importance, a sample showing such extreme values cannot be justifiably represented on a normalised basis, by either N, $\sqrt{N}$ or log N distributions.

7.4. The Use of the Gumbel and Weibull Distributions

One sample (Nylon 10 t.p.i.) has been used to illustrate the use of the Gumbel and Weibull distributions and this is shown in Fig.122 (folded).

As can be seen there are two vertical axes in conjunction with the horizontal axis graduated linearly with N (number of cycles to failure).

One vertical axis (+ 2.5 - -7.5) represents the Gumbel reduced variate y calculated from $y = \log_e (\log_e 1/Q)$, where $Q (= 1 - P)$ is the probability of survival. The other vertical axis represents the probability of survival plotted from the Weibull distribution which has a reduced variate $z = \{- \log_e (1 - P)\}^{\alpha}$ where α is the factor calculated from the skewness of the observed distribution. The Weibull scale has therefore to be calculated for each set of data which makes its use a very arduous task,

FIG 122

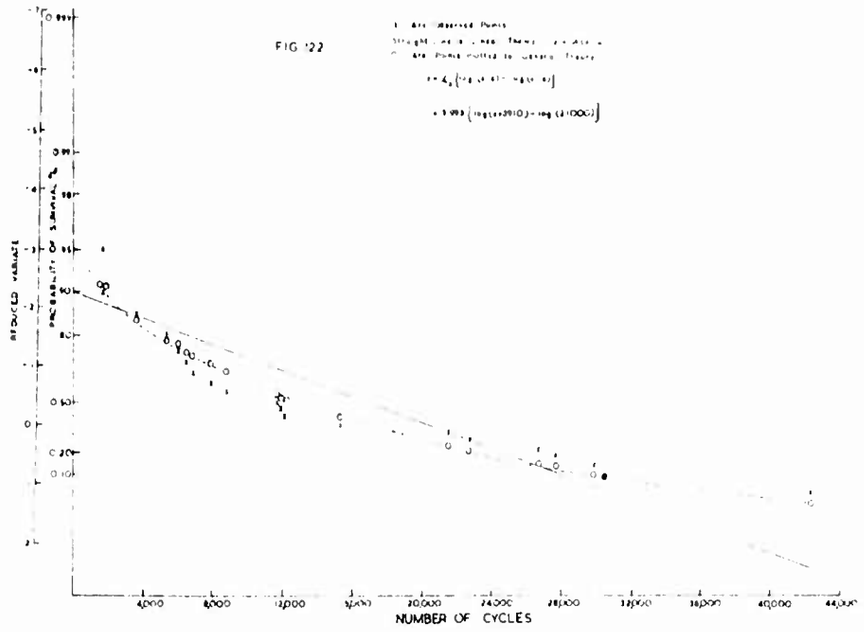

FIG 23

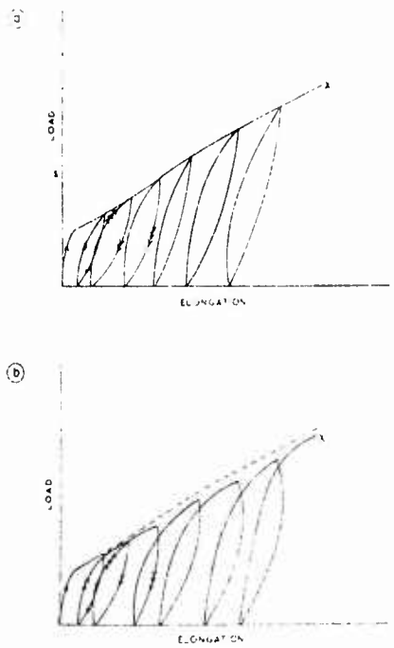

FIG 24

EFFECT OF RATE OF EXTENSION ON ELASTIC RECOVERY

INSTRON TESTS

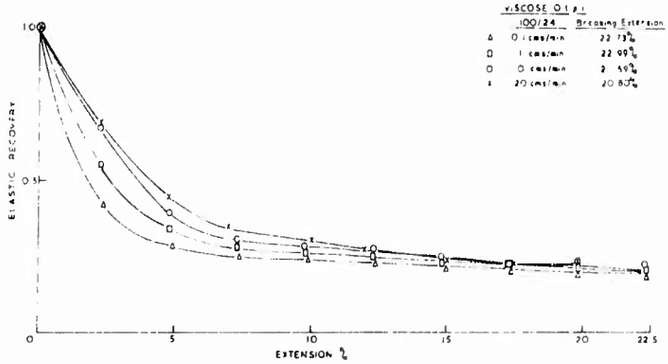

FIG 125

ELASTIC RECOVERY v STRAIN

INSTRON TESTS

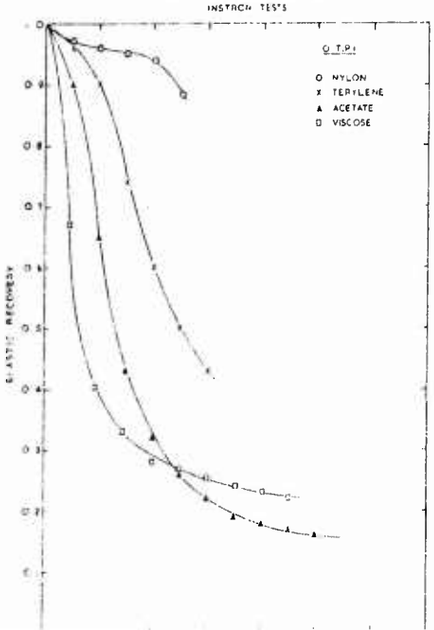

FIG 126

ELASTIC RECOVERY v STRAIN

INSTRON TESTS

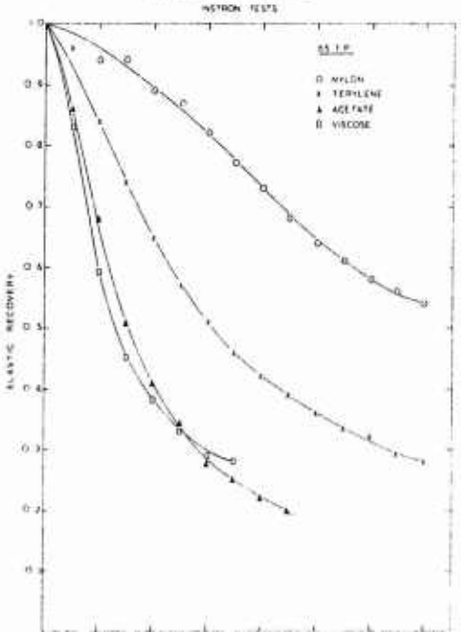

particularly for comparative purposes.

The straight line on the graph represents the Gumbel distribution and is plotted from:

$y = \alpha(x - u)$, where α , u are parameters of slope and location respectively, and are calculated from the observed data.

For the data of the Nylon 10 t.p.i. yarn,

$\alpha = 1.108 \times 10^{-4}$

$u = 20070$

The smooth curve on the graph is a plot of the Weibull distribution

$$y = \alpha_s \left\{ \log (x - \epsilon) - \log (v - \epsilon) \right\}$$

where α_s is the scaling parameter calculated from the skewness of the observed distribution and v, ϵ are dependent on α_s by the gamma function relationships already described.

For the same observed data:

$\alpha_s = 3.993$

$v = 17090$

$\epsilon = -3910$

The observed points are shown to fit the Weibull distribution very closely but the fit to the Gumbel line is not good.

For this particular sample, it may therefore be concluded that the observed data are accounted for reasonably well by assuming that their square roots are normally distributed, but that a better approximation to the observations is afforded by means of the Weibull distribution.

Due to the occurrence of a negative value of ϵ , the Weibull distribution is seen to be invalid for low numbers of cycles, but this does not detract from the fact that the distribution may still be used for the higher ranges.

7.5. Discussion

Although only a limited amount of experimental data has been involved in the statistical approach to the problem of fatigue breakage, three points in particular have emerged as a result of the investigation:

(a) The data as a whole do not give proof that fatigue breaks are normally distributed.

(b) Extreme values play a predominant part and should if possible be accounted for by choice of a suitable distribution.

(c) The use of complex distributions, though a very lengthy procedure, would appear feasible.

The real problem with any statistical test is that a large amount of data is required before any concrete arguments can be vindicated or rejected and in the case of fatigue tests, sometimes of long duration, the data required is not readily available.

CHAPTER 8

FATIGUE BEHAVIOUR AND ITS RELATION WITH ELASTIC RECOVERY PROPERTIES

8.1. Introduction

From previous chapters, and in particular Chapter 5, it is clear that the mechanical dimensions and properties of twisted yarns alter as a fatigue test progresses and an approach which could forecast when a particular yarn is likely to break would be a valuable asset.

When a yarn is subjected to repeated stress, it is not very obvious which mechanical properties are likely to be affected due to cycling and several factors would appear to combine to produce the phenomenological changes which occur.

The creep properties and effect of stress relaxation over very short periods of time during each cycle would seem to have some effect, but one property which probably explains a lot of this behaviour in a test of this nature is that of elastic recovery. By using elastic recovery curves, the stress-strain properties of the yarns are taken into account, since permanent set accruing after each cycle is directly dependent upon recovery from the imposed strain.

By using the elastic recovery curves for the various yarns on a continued basis of strain,recovery, greater strain, less recovery, an empirical approach to the fatigue limit can be made whether that limit involves breakage quickly or slowly. To estimate the recovery after each cycle and to do this on a progressive

basis for large numbers of cycles, is clearly not practicable manually and use has therefore been made of the Atlas computer.

8.2. Simple Theoretical Basis of Predicting Fatigue Behaviour

If we assume that elastic recovery is proportional to strain, then on the first cycle at a certain strain e_1, a certain recovery r_1 will be produced corresponding to a permanent set $e_1(1 - r_1)\,\ell_o$ where ℓ_o is the initial length of the sample. After the first cycle, the take-up mechanism comes into force and the specimen length increases to $\ell_o + e_1(1 - r_1)\,\ell_o$.

On the second cycle the strain (e_2) on the specimen increases to $e_1 + e_1\,(1 + r_1)$ and this will produce a different (slightly smaller) value of elastic recovery (r_2). The total permanent set after the second cycle will be given by $e_2\,(1 - r_2)\,\ell_o$ and in general the permanent set after the n^{th} cycle will be given by $e_n(1 - r_n)\,\ell_o$. The strain for the n^{th} cycle is $e_1 + e_{n-1}(1 - r_{n-1})$.

In this simple theory several assumptions have been made and these are listed below. It has been assumed that:

1. The yarn behaves as if it were undergoing a set of gradually increasing strains, the recoveries from which are identical with those which would be obtained if the specimen were subjected to one cycle at a specified strain. Diagrammatically this is shown in Fig.123.

In case (a) the theoretical load-elongation cycling curve is seen to be continuous from zero strain up to the breaking point, whereas in case (b), successive cycles show that the actual curve

passes through slightly lower values of load for the same strain value. It can be seen, however, that the errors involved in the theory are negligible.

Secondly it has been assumed that the recovery after (say) the n^{th} cycle is dependent only upon the strain and recovery on the $(n-1)^{th}$ cycle and although these values depend on the $(n-2)^{th}$ cycle, no account is taken of the fact that the recovery on the n^{th} cycle may be directly governed by the recovery on the $(n-2)^{th}$ cycle and previous cycles.

Although the errors involved may here be serious it is difficult to find a suitable theoretical treatment to deal with this aspect.

Lastly, the recovery will be governed by the time involved to enable recovery to take place and although this time is maintained as a constant percentage of the cycle (approximately 1/12th), in the fatigue test the effect of this constant time for recovery on different strain levels is difficult to predict, and it may be misleading to say that the time conditions are equivalent for each strain level.

From the observed results for changes in length during the fatigue test, it seems there is a need to separate out the behaviour which occurs principally due to elastic recovery in order to determine the effect which fatigue incurs.

With this in mind and despite the assumptions referred to above, measurement of elastic recovery for each of the samples was carried out. At first, these tests were made on the Instron

tester. Several rates of extension were tried and it was found that the best conditions for testing involved a crosshead speed of 10 cm/min, and the maximum chart speed, namely 100 cm/min. If higher crosshead speeds were used, the inaccuracies due to manual operation at high speeds and the difficulty in measurement of high recoveries (at low strains) became excessive.

The effect of rate of extension on elastic recovery for a viscose 100/24 0 t.p.i. specimen is shown in Fig.124. Five tests were made at each rate of extension and the arithmetic mean of recovery is plotted for each strain level. As is to be expected the breaking extension decreases as the rate of extension increases.

Using a rate of extension of 10 cm/min, the values of elastic recovery for each of the 4 types of yarn with 6 values of twist factor were found. The mean of 5 specimens was taken as the best estimate. Although it was found that twist did not play an appreciable part in determining the values of elastic recovery, the differences observed justified that distinctions should be made between the different twist levels.

Figs.125 and 126 show the differences between the 0 and 65 t.p.i. for the 4 yarns.

In general, it would appear that higher recovery values occur in more highly twisted yarns for each of the 4 types of yarn and this may be expected from theories of the mechanics of twisted yarns. (The closer the coils of a helical spring the greater will be the extent of recovery from an imposed deformation).

The difference between the synthetics and the rayons is certainly very obvious and even more interesting is the significant difference observed between the elastic recovery properties of nylon and Terylene.

Due to the influence of rate of extension upon recovery, it was decided to perform tests for elastic recovery on the fatigue tester itself so that a relationship could be obtained for recovery values which would correspond more nearly to actual fatigue test conditions.

Fortunately, although the original design of the machine did not anticipate it, the fatigue tester was found to be capable of measuring elastic recovery values with a fair degree of accuracy ($\pm$ 5%). By measuring the increase in length $\delta\ell$ after the first cycle at specific strains, the elastic recovery can be calculated from:

$$\text{Elastic recovery} = \frac{\text{Elastic Extension}}{\text{Total Extension}} = 1 - \frac{\delta\ell}{e}$$

where e is the total extension (in units of length).

Difficulties in estimating the recovery at low strains was encountered due to the difficulty of accurate measurement of $\delta\ell$. The error due to the take-up mechanism being a negative one relying on gravity and the sideways movement of the brass rod supporting the bottom yarn jaw, both contributed to produce inaccuracies which swamped the small increase in length which occurred on the first cycle.

Figs.127 and 128 show the curves for the 0 and 65 t.p.i. ranges. A table of values for the 4 yarns with 6 twist ranges is given in the appendix.

It was found that results could be obtained for viscose at

FIG 127

ELASTIC RECOVERY v STRAIN

FATIGUE TESTER RESULTS

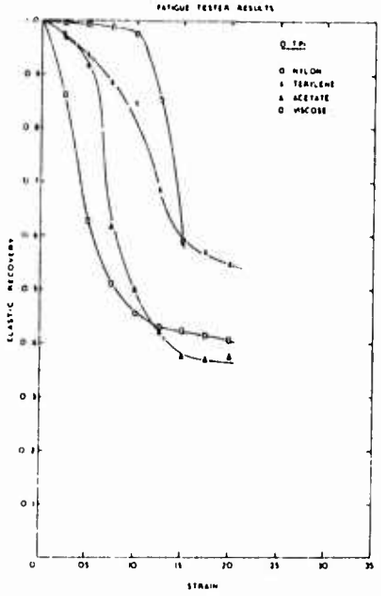

FIG 128

ELASTIC RECOVERY v STRAIN

FATIGUE TESTER RESULTS

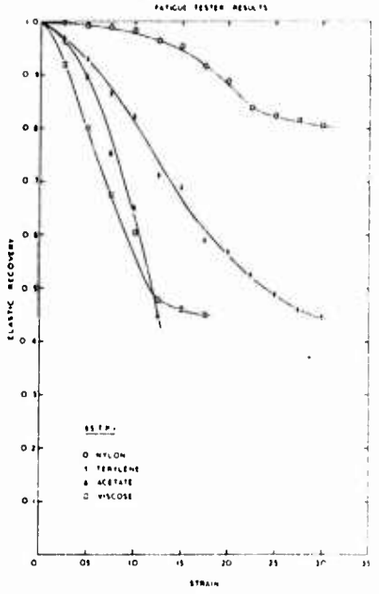

FIG 129

COMPARISON OF OBSERVED AND COMPUTED RESULTS

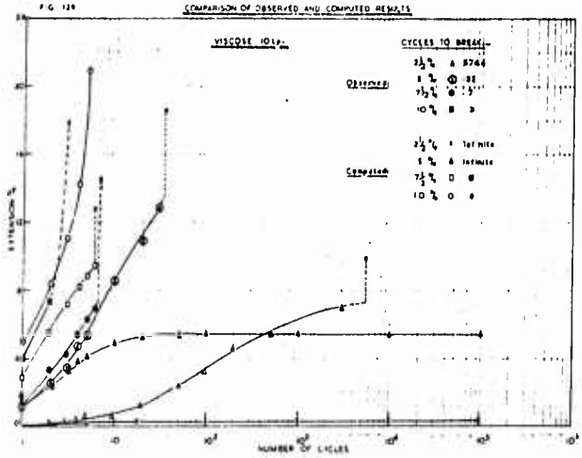

FIG 130

COMPARISON OF OBSERVED AND COMPUTED RESULTS

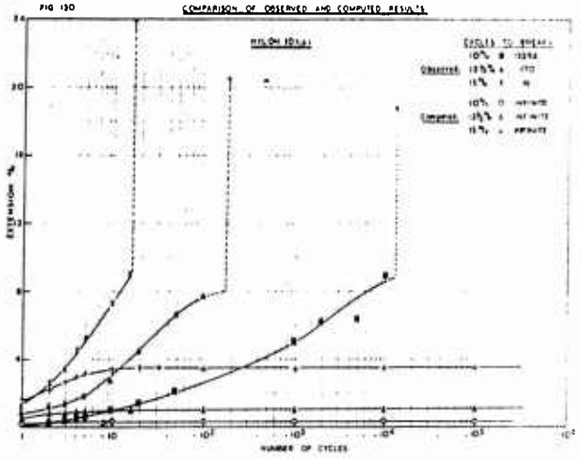

FIG 131

LIGHT CURVE FOR ELASTIC RECOVERY AGAINST STRAIN

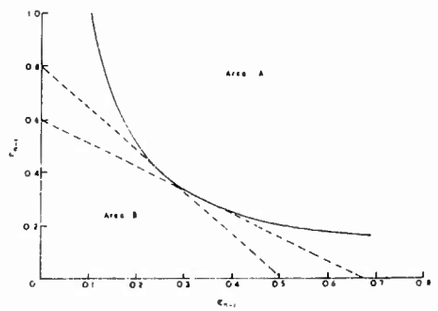

FIG 9.1

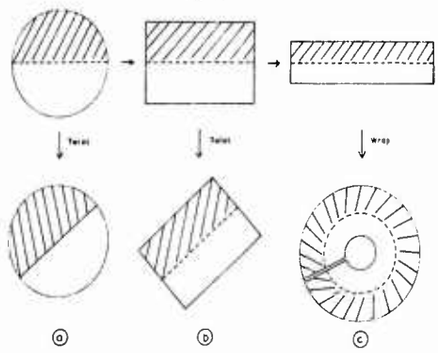

FIG 9.3

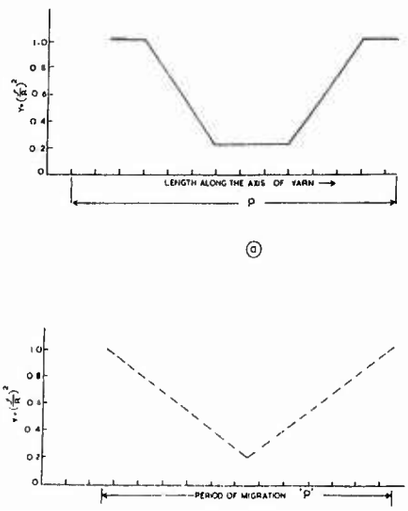

FIG 9.4

the 2.5% level, Acetate at the 5% level, Terylene at the 7.5% and Nylon at the 10% level. Results were obtained at strain levels of 2.5% intervals from zero to 25% for each of the 4 yarns at the 6 ranges of twist. 5 tests were made on each sample.

Values for Terylene at 5% and nylon at 7.5% were taken but found not to be totally reliable and so were discarded.

It must be noted that 25% is the maximum strain possible on the fatigue tester in its present form and so values of elastic recovery from strains higher than this figure could not be achieved; however for the yarns, the breaking extension of which exceeded this region, the shape of the recovery curve is clear and it seems reasonable to extrapolate to 27.5% and 30%. Extrapolation was also carried out at the lower end of the curves where values could not be obtained. In the method of extrapolation account was taken of the results of the Instron tests at lower rates of extension, as well as of the shape of the smooth curve through the observed points.

As is to be expected the breaking extension of the yarns decreases with the increase in rate of extension used on the fatigue tester, and this is particularly noticeable in the cases of viscose and acetate.

Twist in general seems to increase the elastic recovery properties of all the yarns but the effect is more noticeable in nylon and Terylene than the rayons.

The more highly twisted rayons appear to break at lower strains than the lower twisted samples, whereas in the synthetic

yarns this effect is reversed. This is presumably due to the different process of deformation in twisted structures of the two types of yarn.

Having obtained values of elastic recovery from zero strain to the breaking point, it was decided to fit the best curve through these points, so that a systematic theoretical analysis of the fatigue results could be made. By inspection it seemed that a reasonable approximation to the shape of the actual recovery curve could be provided by a third power curve.

By the method of least squares it is possible to find the best cubic by cubic regressional analysis. This method is very tedious and as such an extensive set of data was available, the Atlas computing programme A-1001 was used to profit. Unfortunately, the library programme was originally designed for the Mercury computer and a good deal of time was lost in modifying it to suit Atlas. This standard library programme gives not only the best cubic regressional constants but also the best linear and quadratic forms. It also tabulates an analysis of variance of the observations. Another feature of the programme is that it is possible to "ask" the computer to print out fitted points and this facility has also been used to advantage. The number of required fitted points is restricted to 11, presumably due to output time.

As some of the data contained 13 points, the last 11 points were chosen to incorporate this facility.

Where the range of fatigue testing did not cover low stroke levels, it was decided to use the computer to consider only those

points over which the observed data applied and this was done. However, in 5 cases this meant that only 4 observed points were available and the computer must have 5 points as a minimum, otherwise the degrees of freedom at one stage in the calculation would be zero and using this as a divisor is fatal.

In all,67 sets of data were fed to the computer and the cubic regression parameters were found.

The seven chapter programme fits a cubic polynomial to a set of given data by the method of least squares. The best linear and quadratic forms are also given.

The data are first modified by subtracting the means of the observations $\bar{x}$ and $\bar{y}$. The cubic to be found is then:

$$y = \bar{y} + b\,(x - \bar{x}) + c\left[(x - \bar{x})^2 - \overline{(x - \bar{x})^2}\right] + d\left[(x - \bar{x})^3 - \overline{(x - \bar{x})^3}\right]$$

The three linear equations to determine b, c and d are then formed and solved by straightforward inversion of the matrix. In addition to giving the coefficients b, c and d, the programme prints out an analysis of variance table in standard form to show which regressions are significant. It also gives the variances and covariances of the coefficients and prints a table of the regression line and the 5% confidence limits for specific values of the argument x.

The programme is restricted to 200 points and to not more than 11 fitted points.

In general, for any set of data of 5 points or more, three

linear, three quadratic and three cubic regression parameters were obtained and it was found that at least one (normally a cubic) regression provided reasonably close agreement to the observed data; this statement only holds for the range of extension being covered; outside this range it was found that the cubic term provoked maxima and minima and occasionally points of inflexion, as is to be expected. In several cases the curve was not found to pass through the point (0,1) but it was considered that this was not necessary, provided the curve fitted the data over the range investigated.

Three examples of the closeness of fit of the calculated values are given in Table XXXIII.

TABLE XXXIII

Strain	Viscose 10 tpi.		Terylene 45tpi		Nylon 45 t.p.i.	
	OBS.	Fitted	OBS.	Fitted	OBS.	Fitted
0.000		-	-	-		
0.025	0.904	0.897	-	-		
0.050	0.652	0.679	0.935*	0.935	0.993*	1.006
0.075	0.580	0.546	0.878	0.878	0.990*	0.996
0.100	0.460	0.474	0.845	0.812	0.979	0.977
0.125	0.437	0.441	0.736	0.740	0.978	0.951
0.150	0.429	0.425	0.651	0.668	0.920	0.920
0.175	0.400	0.401	0.559	0.598	0.879	0.887
0.200			0.543	0.536	0.858	0.854
0.225			0.512	0.486	0.803	0.822
0.250			0.456	0.452	0.802	0.795
0.275			0.445*	0.437	0.775*	0.774
0.300			0.435*	0.447	0.763*	0.762

OBS. = Observed Values
Fitted = Fitted Computed Values
* = Extrapolated

The particular regression coefficients used in these cases are shown in Table XXXIV.

TABLE XXXIV

	Coefficient		
	B	C	D
Viscose 10 t.p.i.	-1.928	31.03	-2.45
Terylene 45 t.p.i.	-2.863	2.552	44.92
Nylon 45 t.p.i.	-1.293	-2.006	23.83

The viscose 10 t.p.i. values are intended to show an example of a bad fit, and the other two samples to show a reasonable fit to the observed values. Fortunately the values at the initial stroke where a very accurate value should be used, do agree well, but later agreement is not as good.

Having obtained the regression coefficients, these were then fed in as data into the programme for estimating length and number of cycles to break.

A typical programme, with additional comments is illustrated below.

The programme is designed to print out values of strain, elastic recovery and permanent set at given numbers of cycles.

In order to avoid needless time-wasting, the sets of data were divided so as to make 6 programme tapes, the division being made so that those yarns with an expected life less than 100 cycles were computed together.

PROGRAMME FOR FATIGUE OF TWISTED YARNS

```
JOB
UTTX,BOOTH 2/4
COMPILER MAC
CHAPTERO
Y->1
X->2
E->3
READ(P)
Q=1(1)P
READ(Y1)
JUMP8,0>Y1
READ(X1)
READ(X2)
READ(B)                    <-- INTRODUCTION OF CUBIC PARAMETERS
READ(C)
READ(D)
M=25(25)125                <-- SETTING OF INITIAL STRAIN
E=0.001M
F=E
E1=E-X1
Y=Y1+BE1+CE1E1-CX2+DE1E1E1 <-- CALCULATION OF ELASTIC RECOVERY
X=10E-10EY
PRINT(E)1,8
PRINT(Y)1,8
PRINT(X)1,8
NEWLINE
NEWLINE
I=2(1)100
PRINT(I)6,0
E2=F+X/10
E3=E2-X1
Y=Y1+BE3+CE3E3-CX2+DE3E3E3
X=10E2-10E2Y
PRINT(E2)1,8               <-- PRINTS UP TO 100 CYCLES
PRINT(Y)1,8
PRINT(X)1,8
NEWLINE
JUMP3,E2>0.5
REPEAT
NEWLINE
V=100
W=1
A'=200
G=A'
1)V=V+1
U'=100W+1
```

```
E2=F+X/10
E3=E2-X1
Y=Y1+BE3+CE3E3-CX2+DE3E3E3
X=10E2-10E2Y
JUMP4,V=U'
2)JUMP1,V≠G
PRINT(V)6,0
PRINT(E2)1,8
PRINT(Y)1,8
PRINT(X)1,8
NEWLINE
JUMP3,E2> 0.5
G=G+100W
U=1000W
JUMP1,U≥ G
W=10W
JUMP3,G=100000
G=WA'
JUMP1, 10000> G
4)PRINT(V)6,8
PRINT(E2)1,8
PRINT(Y)1,8
PRINT(X)1,8
NEWLINE
JUMP3,E2> 0.5
JUMP3,G=200000
JUMP1,V≠G
3)REPEAT
REPEAT
8)END
CLOSE
6

0.90017
0.0875
0.002
-0.9696
-51.37
-592.6

0.85425
0.1625
0.003
-2.167
-3.790
66.91

0.92580
0.125
0.001
```

← PRINTS FROM 100 to 1000 AT INTERVALS OF 100 CYCLES

← PRINTS FROM 10^3 to 10^4 at INTERVALS OF 1000 AND ALSO FROM 10^4 TO 10^5 AT INTERVALS OF 10,000

← NUMBER OF SETS OF DATA

← MEAN OBSERVED RECOVERY VALUE
← MEAN OF DATA FOR STRAIN
← MEAN OF $(x - \bar{x})^2$
← COEFFICIENT B
← COEFFICIENT C
← COEFFICIENT D

-2.050
-7.886
304.0

0.92267
0.1375
0.002
-1.996
-7.743
178.4

0.90269
0.150
0.009
-1.293
-2.006
23.83

0.91383
0.1625
0.007
-1.165
-1.552
25.73

xxxZ — END OF DATA INSTRUCTION

8.3. Results

To bring out some of the facts gained from the figures provided by the computer, two sets of results, those for viscose 10 t.p.i. and nylon 10 t.p.i. will be considered.

The values of strain, elastic recovery and permanent set (centimetres) at specific numbers of cycles and for increasing stroke levels are given in Tables XXXV and XXXVI.

Values of the increments in strain, elastic recovery and permanent set (cm) between successive cycles are also given. When the figure zero appears in the increment column, this means that the difference between values on that cycle and the previous one

is less than 10^{-8}. However, as the test was continued until 10^5 cycles and no change occurred it can be assumed that no change greater than 10^{-12} is observed for the greater part of the test. (12 is the maximum number of decimal figures which the computer carries in its calculation).

When the elastic recovery values become negative and the permanent set starts to grow rapidly (clearly not feasible), the computer moves on to the next set of data. This is quite in order and indicates that the yarn theoretically has broken.

It may be noticed that the initial values for elastic recovery at all stroke levels in the case of Viscose 10 t.p.i. differ slightly (up to 2%) from the values tabulated in Table XXXIII. The reasons for this are put down to the fact that in transferring the coefficients and the means of data from one programme to the next, rounding errors are introduced. This argument would particularly apply to the term $\overline{(x - \bar{x})^3}$ which is printed as 0.000 in the cubic regression parameters but which will probably have a value greater than 0.00005 which is not taken into account in the second programme. This is a source of error which is difficult to correct in that the initial cubic regression programme would need to be altered to print out more accurate coefficients, which would in turn alter the parameters used in estimating fatigue life. As this flaw was detected at a very late stage in the work, it was neglected and it is reasonable to assume that the trend and to a great extent the accuracy of the results is maintained.

TABLE XXXV

Computed Values for Viscose 10 t.p.i.

Stroke	No. of Cycles N	Strain S	Elastic Recovery R	Permanent Set P (cm)	ΔS	ΔR	ΔP
2½%	1	.0250	.9123	.0219			
	2	.0272	.8892	.0301	8.0×10^{-3}	2.3×10^{-2}	8.2×10^{-3}
	5	.0285	.8761	.0353	1.3×10^{-4}	1.4×10^{-3}	5.5×10^{-4}
	10	.0286	.8751	.0357	1.6×10^{-6}	1.6×10^{-5}	6.7×10^{-6}
	18	.0286	.8751	.0357	0	0	0
5%	1	.0560	.6943	.1528			
	2	.0653	.6042	.2583	1.5×10^{-2}	9.0×10^{-2}	1.1×10^{-1}
	3	.0758	.5578	.3353	1.1×10^{-2}	4.7×10^{-2}	7.7×10^{-2}
	4	.0835	.5309	.3919	7.7×10^{-3}	2.7×10^{-2}	5.6×10^{-2}
	5	.0892	.5144	.4331	5.6×10^{-3}	1.6×10^{-2}	4.2×10^{-2}
	10	.1010	.4878	.5172	1.1×10^{-3}	2.0×10^{-3}	7.4×10^{-3}
	20	.1034	.4835	.5339	2.9×10^{-5}	5.0×10^{-5}	2.0×10^{-4}
	30	.1034	.4834	.5344	8.4×10^{-7}	1.3×10^{-6}	5.3×10^{-6}
	52	.1034	.4834	.5344	0	0	0
7½%	1	.0750	.5610	.3292			
	2	.1079	.4762	.5652	3.3×10^{-2}	8.5×10^{-2}	2.4×10^{-1}
	3	.1315	.4520	.7207	2.4×10^{-2}	2.4×10^{-2}	1.7×10^{-1}
	4	.1471	.4421	.8206	1.6×10^{-2}	1.0×10^{-2}	1.0×10^{-1}
	5	.1571	.4351	.8872	1.0×10^{-2}	7.0×10^{-3}	6.7×10^{-2}
	10	.1769	.4133	1.0381	2.3×10^{-3}	3.3×10^{-3}	1.9×10^{-2}
	20	.1899	.3888	1.1610	1.1×10^{-3}	2.5×10^{-3}	1.2×10^{-2}
	30	.2130	.3141	1.4610	5.3×10^{-3}	2.1×10^{-2}	8.2×10^{-2}
	33		-ve				

(Cont'd).

TABLE XXXVI (Cont'd)

Stroke	No.of Cycles N	Strain S	Elastic Recovery R	Permanent Set P (cm)	ΔS	ΔR	ΔP
10%	1	.1000	.4897	..5104			
	2	.1510	.4395	.8466	5.1×10^{-2}	5.0×10^{-2}	3.3×10^{-1}
	3	.1847	.4000	1.1079	3.4×10^{-2}	3.9×10^{-2}	2.6×10^{-1}
	4	.2108	.3233	1.4265	2.6×10^{-2}	7.6×10^{-2}	3.2×10^{-1}
	5	.2426	.1340	2.1012	3.2×10^{-2}	1.9×10^{-1}	6.8×10^{-1}
	6		-ve.				
12½%	1	.1250	.4570	.6787			
	2	.1929	.3817	1.1925	6.8×10^{-2}	7.6×10^{-2}	5.2×10^{-1}
	3	.2442	.1209	2.1471	5.2×10^{-2}	2.6×10^{-1}	9.5×10^{-1}
	4		-ve.				
15%	1	.1500	.4402	.8398			
	2	.2340	.1984	1.8755	8.3×10^{-2}	2.4×10^{-1}	1.04
	3		.-ve.				

TABLE XXXVI

Computed Values for Nylon 10 t.p.i.

Stroke	No. of Cycles N	Strain S	Elastic Recovery R	Permanent Set P (cm.)	ΔS	ΔR	ΔP
10%	1	.1000	.9699	.0301			
	2	.1030	.9670	.0340	3.0×10^{-3}	2.9×10^{-3}	3.9×10^{-3}
	3	.1034	.9666	.0345	3.9×10^{-4}	3.7×10^{-4}	5.3×10^{-4}
	4	.1034	.9666	.0346	5.3×10^{-5}	5.4×10^{-5}	7.4×10^{-5}
	5	.1035	.9666	.0346	7.3×10^{-6}	7.5×10^{-6}	1.0×10^{-5}
	8	.1035	.9666	.0346	0	0	0
12½%	1	.1250	.9380	.0775			
	2	.1327	.9250	.0996	7.7×10^{-3}	1.3×10^{-2}	2.2×10^{-2}
	3	.1350	.9210	.1066	2.3×10^{-3}	4.0×10^{-3}	7.0×10^{-3}
	4	.1357	.9198	.1088	7.0×10^{-4}	1.3×10^{-3}	2.3×10^{-3}
	5	.1359	.9193	.1096	2.3×10^{-4}	4.2×10^{-4}	7.5×10^{-4}
	10	.1360	.9191	.1100	1.2×10^{-6}	1.6×10^{-6}	2.9×10^{-6}
	16	.1360	.9191	.1100	0	0	0
15%	1	.1500	.8919	.1620			
	2	.1662	.8575	.2368	1.6×10^{-2}	3.4×10^{-2}	7.4×10^{-2}
	3	.1737	.8410	.2761	7.5×10^{-3}	1.7×10^{-2}	4.0×10^{-2}
	4	.1776	.8322	.2980	4.0×10^{-3}	8.8×10^{-3}	2.2×10^{-2}
	5	.1798	.8274	.3104	2.1×10^{-3}	4.9×10^{-3}	1.3×10^{-2}
	10	.1826	.8211	.3265	1.4×10^{-4}	3.2×10^{-4}	8.4×10^{-4}
	20	.1828	.8207	.3277	7.1×10^{-7}	1.6×10^{-6}	4.2×10^{-6}
	33	.1828	.8207	.3277	0	0	0

Looking at Table XXXV, the results for the viscose yarn, it would appear that at the 2½% stroke level, the yarn elastic recovery reaches a limiting value of 0.8571 after 18 cycles (by a limiting value is meant a value differing from its predecessor by less than 10^{-8}). For the 5% level, this limiting value has dropped to 0.4834 after 52 cycles. The 7½% stroke indicates that a break should have taken place before 33 cycles. If the yarn were merely behaving as a specimen under progressive cumulative extension up to the breaking extension (say 17%), then the break could be forecast after 9 cycles, the permanent set on the 8th cycle being 0.9699 cm, and the stroke 0.75 cm.

In a similar way a break could be expected after the 3rd cycle, when the 10% stroke is used. Referring to the Nylon results in Table XXXVI, the limiting value of elastic recovery for the three stroke levels is 0.9666, 0.9191 and 0.8207 respectively.

Figs.129 and 130 show the differences between observed changes in length and the theoretical changes predicted by the computer, the theoretical curves all lying below the observed values with the exception of Viscose 10 t.p.i. at the 10% stroke where break is predicted (and occurs) after 3 cycles, and at the 7½% stroke where the actual breaking extension is 80% of the theoretical value.

For clarity, the limit values are reproduced in Table XXXVII and the values for number of cycles to break for viscose at stroke levels of 7½% and 12½% are included.

The results for acetate and Terylene are not shown, but their general behaviour is typified by the viscose and nylon results respectively.

TABLE XXXVII

	Stroke	E	E'	N	N'
Viscose 10 t.p.i.	2½%	9.8	2.857	26007	Never
	5%	18.6	10.34	47	Never
	7½%	14.4	Breaks	7	8
	10%	17.8	Breaks	3 or 4	3
	12½%	-	Breaks	2	2
Nylon 10 t.p.i.	10%	18.8	10.346	13274	Never
	12½%	20.5	13.600	170	Never
	15%	24.0	18.277	16	Never
Breaking Extension (Instron Values): Viscose 10 tpi, 16.90% nylon, 10 tpi, 24.75%					

E = Fatigue breaking extension (%)

E' = Computed limiting value of extension (%)

N = Observed Number of cycles to break

N' = Computed number of cycles to break

Even from this very limited set of results it is clear that there appears to be a theoretical limiting extension beyond which the yarn should not go, despite which fact the observed results do show that breakage occurs at large numbers of cycles. It is thus clear that the effect of repeated cycling produces fatigue effects, quite apart from the effects produced by considerations of elastic recovery.

8.4. Study of Theoretical Limits

If it is assumed for simplicity that a linear relationship between recovery and strain exists, then

$$r = 1 + a - be$$

where a and b are constants.

Then the strain after n cycles is given by:

$$\begin{aligned} e_n &= e_1 + e_{n-1}\,(1 - r_{n-1}) \\ &= e_1 + e_{n-1}\,(be_{n-1} - a) \\ &= e_1 - ae_{n-1} + be_{n-1}^{\,2} \end{aligned}$$

If there is a limiting extension,

then $e_n = e_{n-1}$

$$\therefore \quad e_{n-1} = e_1 - ae_{n-1} + be_{n-1}^{\,2}$$

$$\therefore \quad be_{n-1}^{\,2} - (a + 1)\,(e_{n-1}) + e_1 = 0$$

Solving for e_{n-1}

$$e_{n-1} = \frac{(1 + a) \pm \sqrt{(1 + a)^2 - 4be_1}}{2b}$$

At the critical condition:

$$(1 + a)^2 = 4be_1$$

and $e_{n-1} = \frac{1 + a}{2b} = \frac{2e_1}{(1 + a)}$

When $e_1 = 0.1$, $e_{n-1} = \frac{0.2}{1 + a}$

We can now tabulate strain (e_{n-1}) and recovery (r_{n-1}) for various values of a, using the fact that at the critical condition $b = (1 + a)^2/4e_1$.

The hyperbolic curve shown in Fig.131 joins the plotted points for recovery against strain and this shows that if a yarn is strained to a certain value and the recovery value at that strain falls in the area to the right of the hyperbola (Area A), then a limit will occur and no further increase in extension will take place.

Unfortunately the converse does not hold that if the values of recovery for certain strains stay within Area B, then the yarn will break.

Although a linear relationship between strain and recovery has been assumed, there is no reason to assume that quadratic or cubic relationships alter the situation except in dimensions.

8.5. Discussion

Although no conclusive results have been obtained from this simple theoretical study, certain facts in the behaviour of the yarn have come to light and been partially explained. It would seem apparent that to obtain a more accurate estimate of fatigue life, more points would need to be used in estimation of the elastic recovery curves. Another possible way of finding the best fit to these points, apart from polynomial regression, is by interpolation

over the range required.

The discrepancy between the theoretical and the observed values for changes in length certainly indicates that effects other than those due to the property of elastic recovery are taking place during a fatigue test and this is in line with comments made on the change in modulus and geometrical structure which are evident as the test progresses.

CHAPTER 9

CONCLUSIONS

9.1. General Conclusions

The viscoelastic nature of textile materials renders their fatigue properties difficult to assess and the present work represents a small contribution to the overall picture of how fatigue in twisted yarns can be brought on to a quantitative as well as a qualitative basis.

In the initial stages of the work, a constant stroke fatigue tester was designed and found a limited use but as the work has progressed, a second fatigue tester incorporating more facilities has been constructed and has performed the large majority of the testing programme.

From the results of length and stress changes during the course of a test, several conclusions can be drawn. One fact to come out of the data is that the yarns break due to fatigue at comparatively low extensions, in many cases at 60 or 70% of the breaking extension values as measured on the Instron tester. As may be expected, the greater part of the increase in specimen length takes place in the first 100 cycles and after this a linear increase with log (time) is observed up to near the breaking point where a further slight rise is observed.

Stress increases of the order of 100% have been observed between the commencement of a test and breakage, except for the

cases of viscose and acetate at low stress levels, where only a small increase, approximately 10%, is noticed.

The effect of stroke level is very important and the value chosen is one of the major factors which determines the life of the specimen.

An increase in twist factor in general increases the fatigue life of the yarn although this statement cannot be generalised because yarns with twist factors higher than 95 have not been examined. An exception to this rule applies in the case of the low twist raw yarn, where the loose geometrical structure gives rise to progressive filament breakage and where it is likely that a different fatigue mechanism is operative.

From photomicrographs of the fatigued filaments in fractured yarns, it appears that small surface flaws are propagated to cracks and finally to rupture due to repeated stress. The acetate and viscose samples tend to show a fracture perpendicular to the filament axis, whereas in the nylon and to a lesser extent the Terylene samples, it is likely that shearing has taken place either well before the actual break or else at the time of break itself.

A proposed mechanism of fatigue fracture for nylon has been presented but a good deal more information, particularly concerning internal lattice shearing, would be necessary before the proposal could be vindicated.

Statistical assessment of the results of fatigue failures has been undertaken and although in many cases, simple distributions

can be used, it is considered that a complex distribution such as the Weibull is necessary if extreme values are to be explained satisfactorily.

Finally a simple model of a fatigue test, based upon successive values of elastic recovery for the yarns, has been used. Agreement between the observed and the computed values is poor but the possibility of theoretical non-breakage has been realised.

9.2. Proposals for Future Development

With slight modifications, the fatigue tester could be improved still further and additional facilities such as a memory device to enable readings of length and stress at the actual breaking point could be introduced. A deeper investigation into the structural changes which take place as a result of fatigue could be undertaken and particularly in the case of microscopy may prove very fruitful.

To progress further on a statistical or analytical basis, many more results would need to be available and although this would be a valuable step forward, the nature of a fatigue test tends to prohibit large samples.

REFERENCES

1. French, H.J., Fatigue and the Hardening of Steels, Trans.A.S.S.T., 1933.

2. Vidal, G., Sur les methods rapides de determination de la limit de fatigue des metaux et alliages, Recherche Aeronautique, No.34, July 1953.

3. Prot, E.M., Essais de fatigue sous charge progressive, Rev.Met., Dec., 1948

4. Modern Plastics 1947, Vol.1, p.764

5. Engineer, 204: 522-3, O 11 1957

6. Havenhill, R.S., Physics, 7, 179, 136

7. Gough and Parkinson, Trans.Inst.Rubber Industry, 17, 168; 1941

8. Dillon, J.H., Prettyman, I.B. & Hall, G.L., J.Appl.Phys., 15, 309, 1944

9. Springer, A., Rubber Chem. & Technology, 18, 71, 1945.

10. Roberts, G.L., India Rubber World, 100, 31, 1939

11. Owen, O.W., India Rubber World, 114, 4, 07/1946, p.519

12. Goy, R.S. et al., Proc.Inst.Rubber Ind., 1958, p.20-33

13. Bradshaw, W.H., A.S.T.M.Bull., Oct.1945, p.13

14. Buchan, J., B.N.S.Outlook No.3, Summer 1958, and Engineering Materials & Design, March 1959

15. Entwistle et al., Courtaulds Ltd. Publication No.12, 1958

16. Wilson, M.W., Textile Research Journal, 1951, p.47-54

17. Hannel, J.W., Man-made textiles, 36, 424, 10/1959, p.50

18. Himmelfahrt, D., Modern Textiles, 38/04/1957, p.46.

19. Hartley, T.R., Proc.Inst.Rubber Ind., 1956, 32, 2., p.76

20. Wilson, Tappi, 43, 2, 1960, p.129

21. Reeves, E.D., Textile Mercury, 140, 3650, 20/03/1959, p.391

22. Anon., Textile Mercury, 119, 3113, p.787

23. Mallory, G.D., Textile Research Journal, 1951, p.47-54

24. Quintelier, P., Ann.Sci.Text.Belg., 3/09/1960, p.7-29

25. Textile Industries, 119, 03/1955, p.53, 169

26. Redmond, G.B., Trans.Inst.Rubber Ind., 1960, 36, No.3, p.71

27. Hamburger, W. et al., Textile Research Journal, March 1960

28 Lyons, W.J. and Prettyman, I.B., Textile Research Journal 1953, p.917

29. Baker, A., and Swallow, J.E., Royal Aircraft Establishment Tech.Note No.Chem.1355, Nov.1959

30. Swallow, J.E., Royal Aircraft Establishment Tech.Note No. Chem.1381, March 1961

31. Waller, R.C. and Roseveare, W.E., J.Appl.Phys., 1946, p.482

32. Hermans, P.H., J.Phys.Chem., 45, 827, 1941

33. Meredith, R. and Pierce, F.T., J.Textile Inst., 1948, T159

34. Owen, A.E. and Oxley, A.E., J.T.I., 1923, T.18

35. Usenko, V.A. and Murav'eva, K.N., Technology of the Textile Industry USSR, 1960, No.1, p.40

36. Dischka, G., Acta Tech.Acad.Sci.Hungary, 1956, 14, Nos.1 and 2, p.79-93

37. Voyevodin, N.P., Tekstil Prom., 1958, 18, p.59

38. Kargin, A. et al., Dokl.Acad.Nauk, USSR, 1958, p.668

39. Dillon, J.H., American Dyestuff Reporter, 1947, 36, p.385

40. Roff, W.J., Fibres, Plastics & Rubbers, Butterworth Press, 1956

41. Lyons, W.J., Paper presented at the 31st Annual Meeting of the T.R.I., New York City, 16th March 1961

42. Lyons, W.J., Fatigue in textile fibres, Part I, Textile Research Journal, June 1962.

43. Lyons, W.J., Fatigue in textile fibres, Part II, Textile Research Journal, July 1962

44. Lyons, W.J., Fatigue in textile fibres, Part III, Textile Research Journal, September 1962

45. Nandory, G., Variation of the stress-strain properties of cotton tyre cords as a function of twist, Magyar Tekstil, 1959, No.7, p.279

46. Goy, R.S., Effect of cord twist on tyre fatigue, Textile Mercury, 136, 3559, 21/06/1957, p.1053

47. Leblanc, M., Testing a woollen yarn by an apparatus which submits it to repeated extensions, L'Industrie Textile, 1952, July, p.361

48. Fujino et al., A study on fatigue of tyre cords, Series of papers 1955-8, J.Text.Mach.Soc., Japan

49. Okayima, S. and Kikuchi, T., Fatigue and depolymerisation of tyre cord, Chem.Abstr., 1959, No.2, No.9713 from Kogyo Kagaku Zasshi, 60, 756-9, 1957

50. Quintelier, P. and Warzee, M., Effect of form of cabling on the mechanical properties and fatigue resistance of rayon cord for tyres, Ann.Sci.Text.Belg., March 1956, No.1,p.115

51. Wegener, W., Series of article on dynamic testing of cords, 1952 onwards. Influence of various combinations of twist (preliminary and final) on strength and elongation properties of tyre cords, Melliand Textilber., 1960, 41, 7, 804-12

52. Mauvisseau, Contribution to the study of fatigue strength of fibrous high polymers, Bull.Inst.Text. France, 1955, No.51, p.47-78

53. Majmassy, T., The fatigue of yarns caused by repeated stresses. Hung.Tech.Abstr., 1953, 5, No.3, p.81

54. Prevorsek, D. and Lyons, W.J., Analysis and interpretation of of fatigue data in single fibres. T.R.I.Conference, March 1963

55. Frank, F. and Singleton, R.W., A study of factors influencing the tensile fatigue behaviour of yarns, T.R.I.Conference, March 1963

56. El-Behery, H.M.A.E., Ph.D. Thesis, 1959, Manchester University

57. Thakur, V.M., Ph.D. Thesis, 1959, Manchester University

58. Louis Newmark Ltd. publication, Prefect Works, Purley Way, Croydon

59. Lüders, W., Binglers-Polytech.Journal, 155, 18-22, 1860

60. Taylor, G.I., Proc.Roy.Soc., A 145, 1-18, 1934

61. Zaukelies, D.A., J.Appl.Phys., 33, 9, p.2797, 1962

62. Weibull, W. (Ed.), Fatigue testing and analysis of results, Pergamon Press, 1961.

63. Freudenthal, A.M. and Gumbel, E.J., Physical and statistical aspects of fatigue, J.Appl.Mech, 4, 1956

64. Eyring et al., Proc.Nat.Acad.Sci., Washington, 34, 298.

65. Freudenthal and Gumbel, J.Amer.Statistical Soc., 49, 575 (1954)

APPENDIX

APPENDIX

Elastic Recovery Values (Fatigue Tester Results)

VISCOSE

Strain	NOMINAL TURNS PER INCH					
	0	10	20	30	45	65
0.000	1.000	1.000	1.000	1.000	1.000	1.000
0.025	0.864	0.904	0.901	0.932	0.941	0.918
0.050	0.625	0.652	0.668	0.685	0.752	0.798
0.075	0.510	0.580	0.569	0.577	0.641	0.671
0.100	0.456	0.460	0.475	0.498	0.533	0.603
0.125	0.431	0.437	0.469	0.447	0.459	0.475
0.150	0.426	0.429	0.447	0.432	0.440	0.466
0.175	0.419	0.400	0.425	0.406	0.434	0.448
0.200	0.407			0.409		

ACETATE

Strain	NOMINAL TURNS PER INCH					
	0	10	20	30	45	65
0.000	1.000	1.000	1.000	1.000	1.000	1.000
0.025	0.970*	0.965*	0.960*	0.955*	0.960*	0.970*
0.050	0.917	0.902	0.866	0.851	0.864	0.896
0.075	0.618	0.653	0.659	0.697	0.725	0.752
0.100	0.500	0.474	0.507	0.581	0.607	0.650
0.125	0.424	0.359	0.397	0.350	0.340	0.447
0.150	0.378		0.412			
0.175	0.371		0.360			
0.200	0.379					

* Extrapolated value

APPENDIX (Cont'd)

Elastic Recovery Values (Fatigue Tester Results)

NYLON

Strain	NOMINAL TURNS PER INCH					
	0	10	20	30	45	65
0.000	1.000	1.000	1.000	1.000	1.000	1.000
0.025	0.997*	0.995*	0.995*	0.997*	0.995*	0.997*
0.050	0.995*	0.990*	0.990*	0.994*	0.993*	0.994*
0.075	0.990*	0.982*	0.982*	0.990*	0.990*	0.990*
0.100	0.979	0.971	0.971	0.984	0.979	0.984
0.125	0.852	0.944	0.945	0.967	0.978	0.965
0.150	0.588	0.884	0.878	0.912	0.920	0.953
0.175		0.841	0.853	0.856	0.879	0.915
0.200		0.792		0.827	0.858	0.886
0.225		0.725			0.803	0.838
0.250		0.695			0.802	0.824
0.275					0.775*	0.815*
0.300					0.763*	0.805*

TERYLENE

Strain	NOMINAL TURNS PER INCH					
	0	10	20	30	45	65
0.000	1.000	1.000	1.000	1.000	1.000	1.000
0.025	0.975*	0.975*	0.965*	0.970*	0.975*	0.965*
0.050	0.935*	0.945*	0.925*	0.940*	0.935*	0.930*
0.075	0.886	0.906	0.847	0.893	0.878	0.865
0.100	0.846	0.843	0.820	0.857	0.845	0.824
0.125	0.686	0.643	0.745	0.745	0.736	0.711
0.150	0.588	0.532	0.597	0.635	0.651	0.689
0.175	0.570	0.488	0.503	0.552	0.559	0.589
0.200	0.549		0.487	0.539	0.543	0.568
0.225			0.475		0.512	0.522
0.250			0.466		0.456	0.487
0.275			0.455*		0.445*	0.460*
0.300					0.435*	0.445*

* Extrapolated values

Appendix: Personnel and Expenditure

The work described in the report was carried out by Mr. A. J. Booth, B.Sc.Tech., and Mr. O. N. Bose, B.Sc., B.Sc.Tech., under the supervision of Dr. J. W. S. Hearle, M.A., Ph.D., F.Inst.P., F.T.I.

The man-hours spent on the project were approximately 2,000 hours by Mr. Booth, 2,000 hours by Mr. Bose (supported only in part from contract funds) and 200 hours by Dr. Hearle, plus the services of typists and laboratory and workshop technicians.

Material costs were in the region of £200.

The work forms part of a wider programme of work on the mechanics and structure of twisted yarns, being carried on under the direction of Dr. J. W. S. Hearle.
